



# Realistic models of pion-exchange three-nucleon interactions

Steven C. Pieper<sup>1,\*</sup>, V. R. Pandharipande<sup>2,†</sup>, R. B. Wiringa<sup>1,¶</sup>, J. Carlson<sup>3,‡</sup>

<sup>1</sup>*Physics Division, Argonne National Laboratory, Argonne, Illinois 60439*

<sup>2</sup>*Department of Physics, University of Illinois, Urbana, Illinois 61801*

<sup>3</sup>*Theoretical Division, Los Alamos National Laboratory, Los Alamos, New Mexico 87545*

(February 7, 2008)

## Abstract

We present realistic models of pion-exchange three-nucleon interactions obtained by fitting the energies of all the 17 bound or narrow states of  $3 \leq A \leq 8$  nucleons, calculated with less than 2% error using the Green's function Monte Carlo method. The models contain two-pion-exchange terms due to  $\pi N$  scattering in S- and P-waves, three-pion-exchange terms due to ring diagrams with one  $\Delta$  in the intermediate states, and a phenomenological repulsive term to take into account relativistic effects, the suppression of the two-pion-exchange two-nucleon interaction by the third nucleon, and other effects. The models have five parameters, consisting of the strength of the four interactions and the short-range cutoff. The 17 fitted energies are insufficient to determine all of them uniquely. We consider five models, each having three adjustable parameters and assumed values for the other two. They reproduce the observed energies with an rms error  $< 1\%$  when used together with the Argonne  $v_{18}$  two-nucleon interaction. In one of the models the  $\pi N$  S-wave scattering interaction is set to zero; in all others it is assumed to have the strength suggested by chiral effective field theory. One of the models also assumes that the  $\pi N$  P-wave scattering interaction has the strength suggested by effective field theories, and the cutoff is adjusted to fit the data. In all other models the cutoff is taken to be the same as in the  $v_{18}$  interaction. The effect of relativistic boost correction to the two-nucleon interaction on the strength of the repulsive three-nucleon interaction is estimated. Many calculated properties of  $A \leq 8$  nuclei, including radii, magnetic dipole and electric quadrupole moments, isobaric analog energy differences, etc., are tabulated. Results obtained with only Argonne  $v'_8$  and  $v_{18}$  interactions are also reported. In addition, we present results for 7- and 8-body neutron drops in external potential wells.

PACS numbers: 21.10.-k, 21.45.+v, 21.30.+y, 13.75.Cs, 12.40.Qq,

Typeset using REVTeX

## I. INTRODUCTION

One of the primary goals of nuclear physics is to understand the stability, structure, and reactions of nuclei as a consequence of the interactions between individual nucleons. However, these interactions are not known from first principles; they are modeled with parameters to be determined from data. Significant advances have been made during the last decade in the *ab initio* calculation of nuclear properties starting from these realistic models of the nuclear force, which allow us to test the predictions of such models with unprecedented accuracy, and to refine them. With our collaborators, we have carried out a series of many-body calculations of light nuclei [1,2] and nuclear and neutron star matter [3] using a Hamiltonian that contains both two- and three-nucleon potentials. The light nuclei calculations use the Green's function Monte Carlo (GFMC) method and have been demonstrated to give nuclear binding energies for up to eight-body nuclei with a precision of better than 2%. The matter calculations are less accurate but provide important constraints on the Hamiltonian. These calculations have used the Argonne  $v_{18}$  (AV18) model [4] of the two-nucleon interaction,  $v_{ij}$ , and the Urbana IX (UIX) model [5] of the three-nucleon interaction,  $V_{ijk}$ .

The results for light nuclei are summarized in Fig. 1, where we compare the calculated and experimental binding energies for all the ground or narrow, low-lying, excited states of nuclei with up to eight nucleons (neglecting isobaric analog states). In addition to the predictions of the AV18/UIX Hamiltonian, we show the results (most newly calculated for the present paper) of using just the two-body AV18 interaction by itself. We see that AV18 alone predicts some key features of nuclear structure correctly, such as the proper ordering of excited states and the rapid saturation of the binding above  ${}^4\text{He}$ . However, with the exception of  ${}^2\text{H}$ , it underbinds all nuclei, and this failure grows rapidly with increasing  $A$ . With just the two-nucleon force acting, the Borromean nuclei  ${}^6\text{He}$  and  ${}^8\text{He}$  are not stable and the lithium nuclei are only marginally so.

The addition of the UIX model of  $V_{ijk}$  fixes the binding energy of  ${}^3\text{H}$  and  ${}^4\text{He}$  and significantly improves the binding of the p-shell nuclei. However, AV18/UIX still underbinds as  $A$  increases, and also as  $N - Z$  increases. In particular,  ${}^8\text{He}$  is more underbound than  ${}^8\text{Be}$ , indicating a problem with the isospin dependence of this interaction model. The relative stability of the lithium nuclei is improved, but the Borromean helium nuclei are still unbound. Additional calculations of wider, higher-lying, excited states not shown in Fig. 1 indicate another problem with the AV18/UIX model: the underprediction of spin-orbit splittings among spin-orbit partners such as the  $\frac{3}{2}^-$  and  $\frac{1}{2}^-$  states in  ${}^5\text{He}$ .

In this paper we investigate new models of  $V_{ijk}$  that largely correct these failings and give a very good description of the spectrum of light nuclei. Studies of nuclear and neutron star matter with these new models will be reported in a separate paper.

The theory of strong interactions has not yet progressed enough to permit a first-principles determination of the two- and three-nucleon interactions with the accuracy required to calculate nuclear binding energies. The interactions must be determined phenomenologically. Modern, realistic models of  $v_{ij}$  are obtained by fitting the  $\sim 4300$  data below 350 MeV in the Nijmegen  $NN$ -scattering data base [6] with a  $\chi^2 \sim 1$  per degree of freedom. The Nijmegen data base is said to be complete, i.e., the included data determine all the relevant phase shifts and mixing parameters. Thus  $v_{ij}$  fitted to it are well determined and generally give very similar predictions of the properties of three- and four-body nuclei,

as will be discussed below.

In contrast it is much more difficult to construct realistic models of  $V_{ijk}$  by simply fitting three-nucleon scattering data, which is dominated by the pairwise forces. The number of operators that can contribute to  $V_{ijk}$  is very large, and until recently, the number of observables that could both be observed and accurately calculated was small. Recent advances in three-nucleon scattering calculations, based on correlated hyperspherical harmonic [7] and Faddeev [8] methods, and in high-precision  $Nd$  scattering experiments, hold significant promise for testing models of  $V_{ijk}$  in this regime. However, the binding energies and excitation spectra of light nuclei also contain a great deal of information, and are in fact the only current means to investigate  $T = \frac{3}{2}$  forces.

An additional concern is that the  $V_{ijk}$  obtained by fitting nuclear data may depend strongly on the model of  $v_{ij}$  used in the Hamiltonian. The  $V_{ijk}$  will naturally depend upon the chosen  $v_{ij}$  to some extent. For example, two equivalent models of  $v_{ij}$ , related by a unitary transformation, will have different but related  $V_{ijk}$  associated with them [9]. However, combinations of  $v_{ij}$  and  $V_{ijk}$  related by unitary transformations will naturally predict the same observables.

Models of  $V_{ijk}$  based on the elimination of field variables date back to the work of Primakoff and Holstein [10]. The first modern meson-exchange model for nuclear  $V_{ijk}$  was proposed by Fujita and Miyazawa (FM) [11]; it contained only the two-pion-exchange three-nucleon interaction  $V^{2\pi, PW}$  due to scattering of the pion being exchanged between two nucleons by a third nucleon via the P-wave  $\Delta$ -resonance. This interaction is attractive in nuclei and nuclear matter. Later theoretical models, such as Tucson-Melbourne (TM) [12] and Brazil [13] included the  $V^{2\pi, SW}$  due to  $\pi N$  S-wave scattering and  $V^{2\pi, PW}$  from all P-wave scattering. In the recent Texas model these two-pion-exchange contributions to  $V_{ijk}$  have been predicted using chiral symmetry [14]. The FM and later models have similar forms for  $V^{2\pi, PW}$ , but the predicted strength of the long-range part of  $V^{2\pi, PW}$  in the later models is almost twice that in FM.

The main failures of a nuclear Hamiltonian containing only two-nucleon interactions include the underbinding of light nuclei, as discussed above, and an overestimate of the equilibrium density of nuclear matter. An attractive  $V^{2\pi}$  addresses the first failure while making the second worse [15]. The Urbana models of  $V_{ijk}$  contain only two terms, the  $V^{2\pi, PW}$  and a phenomenological, repulsive  $V^R$ . The strengths of the two interactions in the most recent Urbana model, UIX, were obtained by reproducing the energy of  ${}^3\text{H}$  via a GFMC calculation and the density of nuclear matter by approximate variational calculations [5,3]. The repulsive term  $V^R$  in  $V_{ijk}$  is essential to prevent nuclear matter from being too dense and overbound.

The expectation value of the  $NNN$  potential is much smaller than that of the  $NN$  potential in nuclei. For example, the ratio of contributions of the UIX and AV18 potentials in  $A \leq 8$  nuclei is  $< 0.1$  [1,2]. However, the  $V_{ijk}$  gives a relatively much larger contribution to nuclear binding energies due to the significant cancellation between the positive kinetic energy and the negative  $NN$  potential. It is this feature that allows us extract information on  $V_{ijk}$  by studying the spectrum of light nuclei.

In the present work we fit the energies of 17 states of up to eight nucleons, calculated by the GFMC method with  $< 2\%$  error, to construct more realistic models of  $V_{ijk}$ . These models are for use with the AV18  $v_{ij}$ . In addition to the already mentioned  $V^{2\pi, PW}$ ,  $V^{2\pi, SW}$ ,

and  $V^R$  terms, they contain three-pion-exchange rings with  $\Delta$  intermediate states,  $V^{3\pi,\Delta R}$ . All the terms are static; their spin-isospin and spatial dependence is taken from theoretical models, and their strengths are varied to fit the observed energies.

The new models are referred to as ‘‘Illinois’’ models; five versions, Illinois-1 to -5 (designated IL1 to IL5) are presented in this paper. The Hamiltonians using AV18 and these  $V_{ijk}$  are referred to as AV18/IL1, etc. For each model, two to three of the available five parameters were adjusted to fit the binding energies of the 17 states assuming plausible values for the other parameters. The IL1 and IL2 models have short-range cutoffs taken from AV18, while IL3 uses the strength predicted by chiral perturbation theory [14] for  $V_{ijk}^{2\pi}$ , and adjusts the cutoff to fit the energies. IL4 and IL5 are further variations of IL2. The qualities of the fits are good, and the extracted strength parameters have plausible values. This suggests that strengths of additional terms in  $V_{ijk}$  cannot be determined from the data included in the present work. It is also possible that additional terms in  $V_{ijk}$  are weaker than  $V^{2\pi,SW}$  and  $V^{3\pi,\Delta R}$ , which in turn are weaker than the  $V^{2\pi,PW}$  and  $V^R$  considered in the older Urbana models.

Several relativistic effects are contained in the two- and three-nucleon potentials fitted to experimental data. However, the boost correction,  $\delta v(\mathbf{P}_{ij})$ , to the two-body interaction is omitted in nonrelativistic Hamiltonians containing  $v_{ij}$  fitted to the scattering data in the two-nucleon center of mass frame. This many-body effect arises from the motion of the center of mass of the  $ij$  pair of nucleons in the presence of the other nucleons. Initially the boost interaction  $\delta v(\mathbf{P}_{ij})$  is neglected in the GFMC calculations. It is subsequently treated as a first-order perturbation. The contribution of  $\delta v(\mathbf{P}_{ij})$  to the binding energy of light nuclei is nearly proportional to that of  $V^R$ . The final value of the strength of  $V^R$  can be adjusted to reproduce the observed energies when the perturbatively computed  $\delta v(\mathbf{P}_{ij})$  contribution is included.

A brief review of the  $NN$  interaction, including relativistic corrections, is given in Sec. II. The new Illinois models of  $V_{ijk}$  are presented in Sec. III. The GFMC calculations of light nuclei are briefly described in Sec. IV. The nuclear energies calculated with AV18 and its approximation AV8', as well as those including the new Illinois three-nucleon potentials are reported in Sec. V. A number of results obtained with the new Illinois models for the light nuclei, including proton and neutron distribution radii, magnetic and quadrupole moments, and isobaric analog energy differences, are also given in Sec. V. In addition, we report results obtained for drops of 7 and 8 neutrons in an external potential well to provide constraints for energy-density functionals of neutron-rich nuclei [18]. Our conclusions are given in Sec. VI.

## II. THE TWO-NUCLEON INTERACTION

We use the Hamiltonian:

$$H = \sum_i -\frac{\hbar^2}{2m_i} \nabla_i^2 + \sum_{i<j} v_{ij} + \sum_{i<j<k} V_{ijk}, \quad (2.1)$$

containing kinetic, two- and three-nucleon interaction energies. The mass difference between the proton and the neutron is taken into account by letting  $m_i$  be the mass of proton or

neutron according to the isospin of nucleon  $i$ , and both strong and electromagnetic isovector and isotensor terms are included in the  $v_{ij}$ .

The Argonne  $v_{18}$  two-nucleon potential [4] contains  $v^\pi$ , the one-pion-exchange potential with a short-range cutoff,  $v^R$  representing all other strong interaction terms, and  $v^\gamma$ , a very complete treatment of the electromagnetic interaction:

$$v_{ij} = v_{ij}^\pi + v_{ij}^R + v_{ij}^\gamma . \quad (2.2)$$

It can be expressed as a sum:

$$v_{ij} = \sum_p v_p(r_{ij}) O_{ij}^p , \quad (2.3)$$

in which  $O_{ij}^p$  are operators, and  $v_p(r_{ij})$  depend only on the interparticle distance  $r_{ij}$ . The first six operators are the only possible isospin-conserving static ones, i.e., operators independent of the nucleon velocities:

$$O_{ij}^{p=1,6} = (1, \boldsymbol{\sigma}_i \cdot \boldsymbol{\sigma}_j, S_{ij}) \otimes (1, \boldsymbol{\tau}_i \cdot \boldsymbol{\tau}_j) , \quad (2.4)$$

where  $S_{ij}$  is the two-nucleon tensor operator. There are only two isospin-conserving spin-orbit terms linear in the velocities, with operators:

$$O_{ij}^{p=7,8} = \mathbf{L} \cdot \mathbf{S} \otimes (1, \boldsymbol{\tau}_i \cdot \boldsymbol{\tau}_j) , \quad (2.5)$$

where  $\mathbf{L}$  and  $\mathbf{S}$  are the relative angular momentum and the total spin respectively. The above eight terms are unique and able to describe most of the features of the  $NN$  interaction. The long-range parts of  $v_4(r_{ij})$  and  $v_6(r_{ij})$ , associated with the  $\boldsymbol{\sigma}_i \cdot \boldsymbol{\sigma}_j$ ,  $\boldsymbol{\tau}_i \cdot \boldsymbol{\tau}_j$  and  $S_{ij}$ ,  $\boldsymbol{\tau}_i \cdot \boldsymbol{\tau}_j$  operators respectively, are given by the one-pion-exchange potential  $v^\pi$ . In addition there are phenomenological parameterizations of the short- and intermediate-range parts of the  $v_p(r_{ij})$ .

It is necessary to add several smaller terms to the above eight in order to fit the scattering data with a  $\chi^2 \sim 1$ . These include terms dependent quadratically on the velocity, and static and spin-orbit terms breaking the isospin symmetry. In AV18 the quadratic operators are chosen as:

$$O_{ij}^{p=9,14} = (L^2, L^2 \boldsymbol{\sigma}_i \cdot \boldsymbol{\sigma}_j, (\mathbf{L} \cdot \mathbf{S})^2) \otimes (1, \boldsymbol{\tau}_i \cdot \boldsymbol{\tau}_j) ; \quad (2.6)$$

however, in the Paris [19] and Nijmegen [20] models  $\nabla^2$  is used in place of the  $L^2$ .

In addition to the isospin-breaking terms in  $v^\gamma$ , strong-interaction isospin-breaking terms are necessary to reproduce the data. The  $O_{ij}^{p=15-17}$  are isotensors with central,  $\boldsymbol{\sigma}_i \cdot \boldsymbol{\sigma}_j$ , and tensor operators, and the long-range part of  $v_{p=15-17}(r_{ij})$  is determined from the difference of the masses of charged and neutral pions. The isovector term associated with  $O_{ij}^{p=18}$  is necessary to explain the difference in the  $T = 1$ ,  $S = 0$   $pp$  and  $nn$  scattering lengths [4]. The interactions associated with the 18 operators listed above contain all the strong and parts of the electromagnetic interaction. In addition, there are four more operators that appear only in the  $v^\gamma$ . The number of parameters contained in the AV18 model of  $v_{ij}$  is  $\sim 40$ , and all of them are fairly well determined by the  $\sim 4300$  data in the Nijmegen data base.

It is well known that two-nucleon scattering data up to 350 MeV cannot determine the potential  $v_{ij}$  uniquely. In addition to AV18 , there are four other modern models: Reid-93, Nijmegen-I and II [20], and CD-Bonn [21], all of which fit the Nijmegen data base. The five models are different from each other in detail. The Reid-93, Nijmegen-II and AV18 models assume that the interaction in each  $LSJ$  partial wave can be represented by a local potential in that partial wave; in addition the operator structure of the AV18 model given above relates the potentials in all partial waves. In states with total spin  $S = 1$  the local potential in  $LSJ$ - $L'SJ$  coupled waves is expressed as a sum of central, tensor and spin-orbit components. On the other hand, the Nijmegen-I and CD-Bonn models include non-local interactions based on boson-exchange phenomenology.

All the models of  $v_{ij}$  contain one-pion-exchange potentials,  $v^\pi$ , as the long-range part, and phenomenological shorter-range parts. Fortunately the  $v^\pi$  gives the largest contribution to nuclear potential energies, and thus the model dependence of the phenomenological parts has a limited scope. However, the  $v^\pi$  itself is not uniquely predicted by theory. That in the CD-Bonn model is derived assuming pseudoscalar pion-nucleon coupling, and is nonlocal, while that in the other models is essentially local. The deuteron and  $^1S_0$ -scattering wave functions predicted by the five models are compared in Ref. [22]. All the local models predict essentially the same wave functions, however, the two nonlocal models give different wave functions. The main difference is in the  $D$ -state wave function of the deuteron; that predicted by CD-Bonn is smaller at  $r < 2$  fm, while that of Nijmegen-I is close to predictions of local models at all values of  $r$ . The  $S$ -state wave functions of the boson-exchange models, CD-Bonn and Nijmegen-I, are larger than those of the local models at  $r < 1$  fm.

The deuteron elastic-scattering form factors are sensitive to the wave function. The  $A(q^2)$  structure function has been accurately measured, most recently at Jefferson Lab [23,24], and results of the recent measurements of the tensor analyzing power,  $T_{20}(q^2)$ , at Jefferson Lab [25] and NIKHEF [26] are also available. These indicate that the deuteron wave functions calculated from the local potentials are very realistic. They correctly predict the observed data with plausible pair currents [27]. In addition, it has been shown recently [28] that nonrelativistic calculations using local  $v^\pi$  give deuteron wave functions close to those predicted with nonlocal  $v^\pi$  obtained with the pseudovector pion-nucleon coupling, favored by chiral perturbation theories, and relativistic kinetic energy. The corrections of order  $p^2/m^2$ , to the amplitudes of states with large momentum  $p$ , coming from relativistic nonlocalities of  $v^\pi$  and relativistic kinetic energy cancel in this case.

The main assumption we make here is that local models provide an accurate representation of  $v_{ij}$ . It is supported by the observed deuteron form factors mentioned above, and is valid for the  $v^\pi$  as shown in Ref. [28]. The local models also predict essentially the same value (7.63 MeV for Reid-93 and 7.62 MeV for AV18 and Nijmegen-II) of the binding energy of the triton in non-relativistic calculations with no three-nucleon potential [29]. The difference between these values and the observed binding energy of 8.48 MeV is one of the indications for the presence of  $V_{ijk}$  in the Hamiltonian (2.1). The triton energies obtained with the Nijmegen-I and CD-Bonn models, without  $\delta v(\mathbf{P}_{ij})$ , are 7.74 and 8.01 MeV respectively [30]. The energies of the alpha particle predicted by AV18 and Nijmegen-II differ by only 0.28 MeV while those predicted by Nijmegen-I and CD-Bonn models are respectively 0.7 and 2.0 MeV more bound than the AV18 value [30].

Accurate calculations of nuclear matter are not yet practical. Nevertheless the nuclear

matter equation of state has been studied for all five modern potentials with the lowest-order Brueckner-Hartree-Fock method with continuous single-particle energies [31], again without relativistic corrections. The local interactions, Nijmegen-II, Reid-93 and AV18, give similar results, while the most nonlocal CD-Bonn gives the lowest energies. The predicted values of equilibrium  $E_0$  and  $\rho_0$  of symmetric nuclear matter are  $-17.6$  MeV at  $0.27 \text{ fm}^{-3}$  with Nijmegen-II,  $-18.1$  at  $0.27$  with AV18,  $-18.7$  at  $0.28$  with Reid-93,  $-20.3$  at  $0.31$  with Nijmegen-I and  $-22.9$  at  $0.37$  with CD-Bonn, while the empirical values are  $-16$  MeV at  $0.16 \text{ fm}^{-3}$ . The above Brueckner results for AV18 are quite close to the  $E_0 = -18.2$  MeV and  $\rho_0 = 0.3 \text{ fm}^{-3}$  obtained with the variational method using chain summation methods [3]. The triton and  $^4\text{He}$  energies obtained with the nonlocal CD-Bonn interaction are closer to experiment than the predictions of local models, but its predicted nuclear matter properties are farther away.

It has been stressed by Friar [32] that the various representations of  $v^\pi$  are related by unitary transformations. It should be possible to use these transformations to find the appropriate current operators that will explain the deuteron form factors with wave functions predicted by the nonlocal models. These transformations will also generate three-body forces accounting for the difference between energies obtained from local and nonlocal models. Thus the deuteron form factors do not exclude nonlocal representations of  $v_{ij}$ . However, it seems that the simplest realistic models of the nuclear Hamiltonian may be obtained with local  $v_{ij}$ , and fortunately there is much less model dependence in these. In the present work we use the AV18 model of  $v_{ij}$ ; however, the other local models will presumably require similar  $V_{ijk}$ .

The two-nucleon interaction  $v_{ij}$  depends both on the relative momentum  $\mathbf{p} = (\mathbf{p}_i - \mathbf{p}_j)/2$  and the total momentum  $\mathbf{P} = \mathbf{p}_i + \mathbf{p}_j$  of the interacting nucleons. We can express it as:

$$v_{ij} = \tilde{v}_{ij} + \delta v(\mathbf{P}_{ij}) , \quad (2.7)$$

where  $\delta v(\mathbf{P} = 0) = 0$ . The models discussed above give  $\tilde{v}_{ij}$  in the  $\mathbf{P} = 0$ , center of momentum frame. In many calculations the  $\tilde{v}_{ij}$  is used as an approximation to  $v_{ij}$  by neglecting the boost correction  $\delta v(\mathbf{P}_{ij})$ . In fact terms dependent on  $\mathbf{p}$  included in  $\tilde{v}_{ij}$  are of the same order as those in  $\delta v(\mathbf{P}_{ij})$  dependent on  $\mathbf{P}$  [33]. It is essential to include the  $\delta v(\mathbf{P}_{ij})$  to obtain the true momentum dependence of the  $v_{ij}$ . For example, the electromagnetic interaction between two charges, as well as the analogous vector-meson-exchange interaction between two nucleons depends upon  $\mathbf{p}_1 \cdot \mathbf{p}_2 = \frac{1}{4}\mathbf{P}^2 - \mathbf{p}^2$ . The  $\tilde{v}$  includes only the  $\mathbf{p}^2$  term, while the  $\mathbf{P}^2$  term is in  $\delta v$ . The  $\delta v$  is related to  $\tilde{v}$  and its leading term of order  $\mathbf{P}^2$  is given by:

$$\delta v(\mathbf{P}) = -\frac{P^2}{8m^2}\tilde{v} + \frac{1}{8m^2} [ \mathbf{P} \cdot \mathbf{r} \mathbf{P} \cdot \nabla, \tilde{v} ] + \frac{1}{8m^2} [ (\boldsymbol{\sigma}_1 - \boldsymbol{\sigma}_2) \times \mathbf{P} \cdot \nabla, \tilde{v} ] . \quad (2.8)$$

The validity of the above equation, obtained by Friar [34], in classical and quantum relativistic mechanics and in relativistic field theory has been shown in Ref. [33].

The effects of the  $\delta v(\mathbf{P}_{ij})$  on the energies of  $^3\text{H}$  and  $^4\text{He}$  [17] and nuclear matter [3] have been studied for the AV18 model using the variational method. This boost correction gives a repulsive contribution in both cases. It increases the triton energy by  $\sim 0.4$  MeV away from experiment, while the nuclear matter equilibrium  $E_0$  and  $\rho_0$  move to  $-13.7$  MeV at  $0.23 \text{ fm}^{-3}$ , which is closer to the empirical density, but farther from the empirical energy. The VMC studies [17] of  $\delta v(\mathbf{P}_{ij})$  also show that the dominant corrections come from the first



and second terms of Eq.(2.8) and that only the first six operator terms (the static terms) of AV18 give substantial contributions. Accordingly, we ignore the last term of Eq.(2.8) in this paper and evaluate the first two for only the static parts of  $\tilde{v}$ . Furthermore it was shown that the terms arising from the derivatives acting on operators in  $\tilde{v}$  were negligible, so we do not evaluate them here.

### III. ILLINOIS MODELS OF $V_{ijk}$

The Illinois  $V_{ijk}$  are expressed as:

$$V_{ijk} = A_{2\pi}^{PW} O_{ijk}^{2\pi, PW} + A_{2\pi}^{SW} O_{ijk}^{2\pi, SW} + A_{3\pi}^{\Delta R} O_{ijk}^{3\pi, \Delta R} + A_R O_{ijk}^R . \quad (3.1)$$

Their four terms represent the  $V^{2\pi, PW}$ ,  $V^{2\pi, SW}$ ,  $V^{3\pi, \Delta R}$ , and  $V^R$  interactions with strengths  $A_{2\pi}^{PW}$ ,  $A_{2\pi}^{SW}$ ,  $A_{3\pi}^{\Delta R}$ , and  $A_R$ . In the following subsections we give the spin-isospin and spatial operators associated with these interactions and the theoretical estimates of the strengths. In the older Urbana models  $A_{2\pi}^{PW}$  is denoted by  $A_{2\pi}$ ,  $A_R$  by  $U_0$  and the  $V^{2\pi, SW}$  and  $V^{3\pi, \Delta R}$  terms are absent.

#### A. $V^{2\pi, PW}$

The earliest model of  $V^{2\pi, PW}$  is due to Fujita and Miyazawa [11], who assumed that it is entirely due to the excitation of the  $\Delta$ -resonance as shown in Fig. 2a. Neglecting the nucleon and  $\Delta$  kinetic energies we obtain:

$$A_{2\pi}^{PW} = -\frac{2}{81} \frac{f_{\pi NN}^2}{4\pi} \frac{f_{\pi N\Delta}^2}{4\pi} \frac{m_\pi^2}{(m_\Delta - m_N)} , \quad (3.2)$$

$$O_{ijk}^{2\pi, PW} = \sum_{cyc} \left( \{X_{ij}, X_{jk}\} \{\boldsymbol{\tau}_i \cdot \boldsymbol{\tau}_j, \boldsymbol{\tau}_j \cdot \boldsymbol{\tau}_k\} + \frac{1}{4} [X_{ij}, X_{jk}] [\boldsymbol{\tau}_i \cdot \boldsymbol{\tau}_j, \boldsymbol{\tau}_j \cdot \boldsymbol{\tau}_k] \right) , \quad (3.3)$$

$$X_{ij} = T(m_\pi r_{ij}) S_{ij} + Y(m_\pi r_{ij}) \boldsymbol{\sigma}_i \cdot \boldsymbol{\sigma}_j , \quad (3.4)$$

$$Y(x) = \frac{e^{-x}}{x} \xi_Y(r) , \quad (3.5)$$

$$T(x) = \left( \frac{3}{x^2} + \frac{3}{x} + 1 \right) Y(x) \xi_T(r) . \quad (3.6)$$

Here  $\xi_Y(r)$  and  $\xi_T(r)$  are short-range cutoff functions. We note that the one-pion-exchange two-nucleon interaction used in AV18 is given by:

$$v_{ij}^\pi = \frac{1}{3} \frac{f_{\pi NN}^2}{4\pi} m_\pi \boldsymbol{\tau}_i \cdot \boldsymbol{\tau}_j X_{ij} , \quad (3.7)$$

with cutoff functions

$$\xi_Y(r) = \xi_T(r) = (1 - e^{-cr^2}) , \quad (3.8)$$

and  $c = 2.1 \text{ fm}^{-2}$ . The contact,  $\delta$ -function part, of the OPEP is not included in the  $v^\pi$  in Urbana-Argonne models since it is difficult to separate it from the other short-range parts. These functional forms are used in UIX and all the Illinois models.

In all the Illinois models except IL3 the cutoff  $c = 2.1 \text{ fm}^{-2}$  is used and the  $A_{2\pi}^{PW}$  is varied to fit the data, as in UIX. This approximation assumes that the  $\pi N\Delta$  form factor is similar to the  $\pi NN$  form factor. In fact it is likely that the radius of the  $\Delta$ -resonance is larger than that of the nucleon, and thus the  $\pi N\Delta$  form factor is softer than the  $\pi NN$ . In this case use of the  $T(x)$  and  $Y(x)$  functions from  $v_{ij}$  in  $V^{2\pi, PW}$  would lead to an underestimation of  $A_{2\pi}^{PW}$ . In the IL3 model we use a value of  $A_{2\pi}^{PW}$  typical of the Tucson, Brazil, and Texas models [12–14] and vary the cutoff parameter  $c$  in  $V_{ijk}$  to fit the data.

Using the observed values of  $m_\Delta$  and  $f_{\pi N\Delta}^2/4\pi \sim 0.3$ , Eq.(3.2) predicts that  $A_{2\pi}^{PW} \sim -0.04 \text{ MeV}$ . With the cutoffs from  $v_{ij}$ , the  $V^{2\pi, PW}$  of this strength gives a contribution of  $\sim -3 \text{ MeV}$  to the energy of  ${}^3\text{H}$ . It is much larger than the  $-0.9$  to  $-0.6 \text{ MeV}$  estimated by Faddeev calculations [35,36] that include explicit  $\Delta$  degrees of freedom and  $NN \rightleftharpoons N\Delta$  transition potentials [37]. A part of the difference is probably due to the neglect of kinetic energies of the nucleons and  $\Delta$  in the energy denominator in Eq.(3.2). Neglecting the momenta of the nucleons before the pion emission, the energy denominator in Eq.(3.2) should be  $m_\Delta - m_N + q_\pi^2(1/2m_\Delta + 1/2m_N)$ , where  $\mathbf{q}_\pi$  is the momentum of the first pion in Fig. 2a. The average momenta of pions exchanged in interactions between nucleons in nuclei is  $\sim 500 \text{ MeV}/c$  [38,39], for which Eq.(3.2) underestimates the denominator by  $\sim 40\%$ . It thus appears likely that Eq.(3.2) overestimates the strength of  $V^{2\pi, PW}$  via the  $\Delta$ -resonance significantly.

The other models of  $V_{ijk}$  start from the observed pion-nucleon scattering amplitude, and use current algebra and PCAC constraints, or chiral symmetry, to extrapolate to the off-mass-shell pions responsible for the  $V^{2\pi}$ . In this way they include the contributions of all the  $\pi N$  resonances, as well as that of  $\pi N$  S-wave scattering to the  $V^{2\pi}$ . The TM  $V^{2\pi}$  has been cast in the form of Eq.(3.1) in Ref. [15]. It contains the term  $V^{2\pi, PW}$  with the operator  $O_{ijk}^{2\pi, PW}$  and the strength  $A_{2\pi}^{PW} = -0.063 \text{ MeV}$ . The strength  $A_{2\pi}^{PW}$  is proportional to the parameter  $b$  in the  $\pi N$  scattering amplitude, and the values of  $b$  in various models have been tabulated by Friar et al. [14]. The Texas model has the largest value of  $b$  corresponding to  $A_{2\pi}^{PW} = -0.09$ . These strengths are much larger than  $-0.04$  estimated with the simple Fujita-Miyazawa model presumably because of the additional contributions included. However, the nucleon and resonance kinetic energies are neglected in the later models, as in the FM, therefore their estimate of the strength of  $V^{2\pi, PW}$  may be too large in magnitude. Another concern is that the  $\pi N$  scattering amplitude used in these models considers only pions of momenta less than  $m_\pi$  [14]. They play a much smaller role in nuclear binding than those with momenta  $\sim 500 \text{ MeV}/c$ .

The factor of  $1/4$  in the second term of  $O_{ijk}^{2\pi, PW}$  [Eq.(3.3)], containing the product of commutators, is due to the spin and isospin of the  $\Delta$  being  $3/2$ . In the TM and later models the strength of this term is proportional to the constant  $d$  whose values have also been tabulated by Friar et al. [14]. The value of  $d/b$  is  $0.29$  in the latest Texas model, however, the ratio of the expectation values of the commutator and anticommutator terms of  $O_{ijk}^{2\pi, PW}$  is very constant across all the light nuclei studied in this work, and hence this factor cannot be determined from the data considered here. We continue to use the Fujita-Miyazawa value of  $0.25$  in this work for simplicity.

## B. $V^{2\pi,SW}$

The form of the  $V^{2\pi,SW}$ , due to  $\pi N$  S-wave scattering illustrated in Fig. 2b, in the TM model is:

$$B(\mathbf{r}_{ij}, \mathbf{r}_{jk}) \{ \boldsymbol{\tau}_i \cdot \boldsymbol{\tau}_j, \boldsymbol{\tau}_j \cdot \boldsymbol{\tau}_k \} \{ (S_{ij} + \boldsymbol{\sigma}_i \cdot \boldsymbol{\sigma}_j), (S_{jk} + \boldsymbol{\sigma}_j \cdot \boldsymbol{\sigma}_k) \} , \quad (3.9)$$

The  $B(\mathbf{r}_{ij}, \mathbf{r}_{jk})$  contains several terms as given in Ref. [15]. We omit the short-range terms containing the  $Z'_0$  functions, whose validity has been questioned recently [14], and retain only the term with pion-exchange-range functions  $Z'_1$ . These functions are given in Eqs.(A17,A18) of Ref. [15]. The function  $Z'_1$  is trivially related to the functions  $Y(x)$  and  $T(x)$  in  $v_{ij}^\pi$  [Eqs.(3.4-3.7)], and the  $Z'_1$  contribution to  $V^{2\pi,SW}$  is expressed as:

$$A_{2\pi}^{SW} = \left( \frac{f_{\pi NN}}{4\pi} \right)^2 a' m_\pi^2 , \quad (3.10)$$

$$O_{ijk}^{2\pi,SW} = \sum_{cyc} Z(m_\pi r_{ij}) Z(m_\pi r_{jk}) \boldsymbol{\sigma}_i \cdot \hat{\mathbf{r}}_{ij} \boldsymbol{\sigma}_k \cdot \hat{\mathbf{r}}_{kj} \boldsymbol{\tau}_i \cdot \boldsymbol{\tau}_k , \quad (3.11)$$

$$Z(x) = \frac{x}{3} [Y(x) - T(x)] . \quad (3.12)$$

The values of the parameter  $a'$  are listed in Ref. [14]; they vary from  $-0.51/m_\pi$  to  $-1.87/m_\pi$  in the recent models. The TM value  $a' = -1.03/m_\pi$  gives  $A_{2\pi}^{SW} \sim -0.8$  MeV. The  $V^{2\pi,SW}$  gives rather small contributions to nuclear energies, and it is difficult to extract its strength  $A_{2\pi}^{SW}$  from nuclear data. In model IL1 we neglect this term, while in all other models it is assumed to have the theoretically plausible strength of  $-1$  MeV.

## C. $V^{3\pi,\Delta R}$

The present model of  $O_{ijk}^{3\pi,\Delta R}$  is based on the three-pion-exchange ring diagrams shown in Figs. 2c,d having only one  $\Delta$  at a time in the intermediate states. The  $V^{3\pi,\Delta R}$  is approximated with the sum of  $V_1^{3\pi,\Delta R}$  and  $V_2^{3\pi,\Delta R}$ , which respectively denote the sums of diagrams 2c and 2d. After neglecting the kinetic energies of the nucleons and the  $\Delta$  in the intermediate states, diagram 2c gives:

$$V_{1,ijk}^{3\pi,\Delta R} = \sum_{cyc} \frac{1}{(m_\Delta - m_N)^2} [v_{\Delta N \rightarrow NN}^\pi(ik) v^\pi(jk) v_{NN \rightarrow \Delta N}^\pi(ij) + j \rightleftharpoons k] , \quad (3.13)$$

where  $v_{NN \rightarrow \Delta N}^\pi(ij)$ , for example, denotes the one-pion-exchange transition potential [37] exciting the nucleon  $i$  to the  $\Delta$ -resonance state, and  $j \rightleftharpoons k$  denotes the term obtained by interchanging  $j$  and  $k$  in the previous term. The above  $V_1^{3\pi,\Delta R}$  can be reduced to a three-nucleon operator by eliminating the  $N \rightleftharpoons \Delta$  transition spin and isospin operators denoted by  $\mathbf{S}, \mathbf{S}^\dagger, \mathbf{T}$ , and  $\mathbf{T}^\dagger$  using the generalized Pauli identities:

$$\mathbf{T}^\dagger \cdot \mathbf{T} = 2 , \quad (3.14)$$

$$\mathbf{T}^\dagger \times \mathbf{T} = -\frac{2}{3} i \boldsymbol{\tau} , \quad (3.15)$$

$$\mathbf{T}^\dagger \cdot \mathbf{A} \mathbf{T} \cdot \mathbf{B} = \frac{2}{3} \mathbf{A} \cdot \mathbf{B} - \frac{1}{3} i \boldsymbol{\tau} \cdot \mathbf{A} \times \mathbf{B} , \quad (3.16)$$

for the transition isospin operators. The transition spin operators also obey the same identities with  $\boldsymbol{\tau}$  replaced with  $\boldsymbol{\sigma}$ . It is useful to reduce the  $V_1^{3\pi,\Delta R}$  further by eliminating all the terms quadratic in either  $\boldsymbol{\tau}_l$  or  $\boldsymbol{\sigma}_l$  ( $l = i, j, k$ ) with the Pauli identity:

$$\boldsymbol{\sigma} \cdot \mathbf{A} \boldsymbol{\sigma} \cdot \mathbf{B} = \mathbf{A} \cdot \mathbf{B} + i \boldsymbol{\sigma} \cdot \mathbf{A} \times \mathbf{B} , \quad (3.17)$$

for  $\boldsymbol{\sigma}$  and  $\boldsymbol{\tau}$  operators. The resulting  $V_1^{3\pi,\Delta R}$  contains very many terms which can be organized in the following way:

$$V_{1,ijk}^{3\pi,\Delta R} = A_{3\pi}^{\Delta R} O_{1,ijk}^{3\pi,\Delta R} , \quad (3.18)$$

$$A_{3\pi}^{\Delta R} = \left( \frac{1}{3} \frac{f_{\pi NN}^2}{4\pi} m_\pi \right)^3 \frac{f_{\pi N\Delta}^2}{f_{\pi NN}^2} \frac{1}{(m_\Delta - m_N)^2} , \quad (3.19)$$

$$O_{1,ijk}^{3\pi,\Delta R} = 6 \left( S_\tau^I S_\sigma^I + A_\tau^I A_\sigma^I \right) + 2 \sum_{cyc} \left( S_\sigma^I S_{\tau,ijk}^D + S_\tau^I S_{\sigma,ijk}^D + A_\tau^I A_{\sigma,ijk}^D + S_{\tau,ijk}^D S_{\sigma,ijk}^D \right) . \quad (3.20)$$

The letters  $S$  and  $A$  denote operators that are symmetric and antisymmetric under the exchange of  $j$  with  $k$ . Subscripts  $\tau$  and  $\sigma$  label operators containing isospin and spin-space parts respectively, while superscripts  $I$  and  $D$  indicate operators that are independent or dependent on the cyclic permutation of  $ijk$ . The  $S^I$  and  $A^I$  would be more properly written with  $ijk$  subscripts, but because they are independent of the ordering of  $ijk$ , we omit them here for brevity. The isospin operators are:

$$S_\tau^I = 2 + \frac{2}{3} (\boldsymbol{\tau}_i \cdot \boldsymbol{\tau}_j + \boldsymbol{\tau}_j \cdot \boldsymbol{\tau}_k + \boldsymbol{\tau}_k \cdot \boldsymbol{\tau}_i) = 4P_{T=3/2} , \quad (3.21)$$

$$A_\tau^I = \frac{1}{3} i \boldsymbol{\tau}_i \cdot \boldsymbol{\tau}_j \times \boldsymbol{\tau}_k = \frac{1}{6} [\boldsymbol{\tau}_i \cdot \boldsymbol{\tau}_j, \boldsymbol{\tau}_j \cdot \boldsymbol{\tau}_k] , \quad (3.22)$$

$$S_{\tau,ijk}^D = \frac{2}{3} \boldsymbol{\tau}_j \cdot \boldsymbol{\tau}_k , \quad (3.23)$$

$$A_{\tau,ijk}^D = 0 , \quad (3.24)$$

where we have indicated that  $S_\tau^I$  is a projector onto isospin 3/2 triples (see the discussion at the end of this subsection), and that  $A_\tau^I$  has the same structure as the commutator part of  $V^{2\pi,PW}$ . The spin-space operators have many terms, and are listed in the Appendix. In addition to the spin operators, they contain the functions  $T(x)$  and  $Y(x)$  in the  $v^\pi$ . The interaction  $V_1^{3\pi,\Delta R}$  has to be symmetric under the exchange of  $i, j$ , and  $k$ ; therefore products of  $S$ - and  $A$ -type operators are not allowed.

The  $V_2^{3\pi,\Delta R}$ , obtained from diagram d in Fig.2, after neglecting the kinetic energies, is given by:

$$V_{2,ijk}^{3\pi,\Delta R} = \sum_{cyc} \frac{1}{(m_\Delta - m_N)^2} [v_{N\Delta \rightarrow NN}^\pi(ik) v_{\Delta N \rightarrow N\Delta}^\pi(jk) v_{NN \rightarrow N\Delta}^\pi(ij) + j \rightleftharpoons k] , \quad (3.25)$$

After appropriate reductions it can be cast in the form of  $V_1^{3\pi,\Delta R}$  as follows:

$$V_2^{3\pi,\Delta R} = A_{2,3\pi}^{\Delta R} O_{2,ijk}^{3\pi,\Delta R} , \quad (3.26)$$

$$A_{2,3\pi}^{\Delta R} = A_{3\pi}^{\Delta R} \frac{f_{\pi N\Delta}^2}{f_{\pi NN}^2} , \quad (3.27)$$

$$O_{2,ijk}^{3\pi,\Delta R} = \frac{8}{3} S_\tau^I S_\sigma^I + \frac{2}{3} A_\tau^I A_\sigma^I - \frac{4}{9} \sum_{cyc} \left( S_\sigma^I S_{\tau,ijk}^D + S_\tau^I S_{\sigma,ijk}^D + A_\tau^I A_{\sigma,ijk}^D - \frac{1}{2} S_{\tau,ijk}^D S_{\sigma,ijk}^D \right) . \quad (3.28)$$

The  $V_1^{3\pi,\Delta R}$  and  $V_2^{3\pi,\Delta R}$  are combined using  $f_{\pi N\Delta}^2 \sim 4f_{\pi NN}^2$  to obtain:

$$V_{ijk}^{3\pi,\Delta R} = A_{3\pi}^{\Delta R} \left( O_{1,ijk}^{3\pi,\Delta R} + 4O_{2,ijk}^{3\pi,\Delta R} \right) = A_{3\pi}^{\Delta R} O_{ijk}^{3\pi,\Delta R} , \quad (3.29)$$

$$O_{ijk}^{3\pi,\Delta R} = \frac{50}{3} S_\tau^I S_\sigma^I + \frac{26}{3} A_\tau^I A_\sigma^I + \frac{2}{9} \sum_{cyc} \left( S_\sigma^I S_{\tau,ijk}^D + S_\tau^I S_{\sigma,ijk}^D + A_\tau^I A_{\sigma,ijk}^D + 13 S_{\tau,ijk}^D S_{\sigma,ijk}^D \right) . \quad (3.30)$$

The strengths of the terms independent of cyclic permutations are larger than those which depend upon them. Therefore we use the simpler  $V^{3\pi,\Delta R}$  obtained by neglecting them, i.e. with the approximate operator:

$$O_{ijk}^{3\pi,\Delta R} \approx \frac{50}{3} S_\tau^I S_\sigma^I + \frac{26}{3} A_\tau^I A_\sigma^I . \quad (3.31)$$

The value of  $A_{3\pi}^{\Delta R}$  estimated from the observed values of the constants, and neglecting the kinetic energies, is  $\sim 0.002$  MeV. In all the Illinois models the  $A_{3\pi}^{\Delta R}$  is determined by fitting the nuclear energies.

The  $V^{3\pi,\Delta R}$  has an interesting dependence on the total isospin  $\mathbf{T}_{tot}$  of the three interacting nucleons. The  $S_\tau^I$  can be written as:

$$\mathbf{T}_{tot} = \frac{1}{2} (\boldsymbol{\tau}_i + \boldsymbol{\tau}_j + \boldsymbol{\tau}_k) , \quad (3.32)$$

$$S_\tau^I = \frac{4}{3} T_{tot}^2 - 1 . \quad (3.33)$$

Therefore the first term of  $V^{3\pi,\Delta R}$  is zero in triplets having  $T_{tot} = 1/2$ , i.e., in  $d+N$  channels as well as in the  $A = 3, 4$  bound states. In contrast  $A_\tau^I$  is zero in  $T_{tot} = 3/2$  states. It is therefore possible to extract the strength of this interaction from the data even though it is much weaker than the  $V^{2\pi}$ .

#### D. $V^R$

The pion-exchange three-nucleon interactions are attractive, and lead to significant overbinding and large equilibrium density of nuclear matter. Therefore there must be other three-nucleon interactions to compensate the attraction from  $V^{2\pi}$  in nucleon matter at large density. In Faddeev calculations of the triton including  $\Delta$  excitations [35,36], the attraction from processes included in  $V^{2\pi}$  is more than cancelled by “dispersion” terms which describe the modification of the contribution of the two-pion-exchange  $\Delta$ -box diagrams to  $v_{ij}$  due to the presence of the third nucleon  $k$ . Such repulsive terms also occur in the variational theory in which  $\Delta$ -excitations are included via transition correlation operators [40]. The  $V^R$  term in the Urbana models of  $V_{ijk}$  was designed to approximate these effects. It is retained in the Illinois models with the simple spin-isospin independent operator:

$$O_{ijk}^R = \sum_{cyc} T^2(m_\pi r_{ij}) T^2(m_\pi r_{jk}) , \quad (3.34)$$

Results of the Faddeev calculations [35,36] indicate that the  $\Delta$ -effects not included in the  $V^{2\pi}$  add  $\sim 1$  MeV to the energy of the triton. The value of the strength  $A_R$  required to obtain a contribution of  $\sim 1$  MeV from the  $V^R$  to the triton energy is  $\sim 0.004$  MeV for a  $T(r)$  with a cutoff  $c = 2.1$  fm $^{-2}$ . In models IL1-4 the  $A_R$  is determined by fitting nuclear energies.

### E. $V_{ijk}^*$

Most calculations of light nuclei use the simpler Hamiltonian obtained by approximating the  $v_{ij}$  in Eq.(2.1) by the  $\tilde{v}_{ij}$ . The more accurate Hamiltonian:

$$H^* = \sum_i -\frac{\hbar^2}{2m_i} \nabla_i^2 + \sum_{i<j} (\tilde{v}_{ij} + \delta v(\mathbf{P}_{ij})) + \sum_{i<j<k} V_{ijk}^* , \quad (3.35)$$

contains the boost correction to the two-nucleon interaction. This correction  $\delta v(\mathbf{P}_{ij})$  is of first order in  $P_{ij}^2$ , and therefore its contribution is calculated as a first-order perturbation in wave functions generated by a nonrelativistic Hamiltonian that gives the same final energy as  $H^*$ . In light nuclei the expectation values of  $\delta v$  and  $V^R$  are nearly proportional to each other [16,17]. Therefore the energies of light nuclei, calculated with the simpler  $H$  can be reproduced with the  $H^*$  using:

$$V_{ijk}^* = A_{2\pi}^{PW} O_{ijk}^{2\pi,PW} + A_{2\pi}^{SW} O_{ijk}^{2\pi,SW} + A_{3\pi}^{\Delta R} O_{ijk}^{3\pi,\Delta R} + A_R^* O_{ijk}^R . \quad (3.36)$$

which differs from  $V_{ijk}$  only in the strength of  $V^R$ . For  $T(r)$  with cutoff  $c = 2.1 \text{ fm}^{-2}$  the strength  $A_R^*$  in  $V_{ijk}^*$  is smaller than  $A_R$  by  $\sim 0.002 \text{ MeV}$ . The proportionality of  $\delta v$  and  $V^R$  contributions appears only in bound light nuclei. In nuclear matter the  $\delta v$  contribution increases more slowly with density than that of  $V^R$ , and in neutron drops the  $\delta v$  gives a relatively larger contribution. Therefore it is necessary to use the  $H^*$  [3] in these systems.

### F. The Illinois Model-5

This model is meant to test the sensitivity of nuclear energies to the spatial shape of  $V^R$ . Here we assume that:

$$V_{ijk}^R = 0.002 O_{ijk}^R + A_W \prod_{cyc} W(r_{ij}) , \quad (3.37)$$

where  $W(r)$  is a modified Woods-Saxon function that has zero-derivative at the origin:

$$W(r) = \frac{1}{1 + e^{(r-r_W)/a_W}} \left[ 1 + \frac{r/a_W}{1 + e^{r_W/a_W}} \right] , \quad (3.38)$$

with  $r_W = 1.0 \text{ fm}$  and  $a_W = 0.2 \text{ fm}$ . The first term of this  $V^R$  is meant to take into account the contribution of  $\delta v$  omitted from the simpler  $H$ , and the second corresponds to the phenomenological three-nucleon repulsion.

### G. Potential Parameters

The parameters of the Illinois potentials were determined by fitting the observed energies of  $3 \leq A \leq 8$  nuclei. The simpler Hamiltonian  $H$  was used, and a total of 17 ground or excited states with widths less than 200 keV were considered. Table I presents the parameters of the new potentials, and for comparison those of UIX [1]. The properties of light nuclei

calculated from Hamiltonians including the AV18  $v_{ij}$  and the new  $V_{ijk}$  are presented below in Sec. V. In addition to the various strengths, Table I gives the value,  $c$ , of the cutoff constant in Eq.(3.8) which is used in all the four terms of  $V_{ijk}$ .

As mentioned earlier, this data set cannot determine all five parameters of the Illinois  $V_{ijk}$ . At most three parameters were varied for each model, and plausible values are assumed for the others. These assumed values are marked with an asterisk in Table I. There is a substantial cancellation between the contributions of  $V^{2\pi, PW}$  and  $V^R$  in the nuclear binding energies. Therefore one can make correlated changes in the  $A_{2\pi}^{PW}$  and  $A_R$ , as in models IL2 and IL4, without significantly spoiling the fit. Presumably nuclear matter calculations with these models can help to further constrain the parameters.

As will be discussed later, the contributions of  $V^{2\pi, SW}$  and  $V^{2\pi, PW}$  are in a fairly constant ratio for the light nuclei considered here, and thus we cannot uniquely determine both  $A_{2\pi}^{SW}$  and  $A_{2\pi}^{PW}$ . IL1 assumes that  $A_{2\pi}^{SW} = 0$ , while in all other models  $A_{2\pi}^{SW} = -1$  MeV as in modern chiral-perturbation-theory potentials [14]. The  $A_{2\pi}^{PW}$  in IL2 is less than that in IL1 by  $\sim 4\%$  to compensate for the  $V^{2\pi, SW}$  contribution. All models other than IL3 have the same cutoff,  $c$ , as in AV18 and UIX and have  $A_{2\pi}^{PW}$  of the same order of magnitude as the Urbana models. This  $A_{2\pi}^{PW}$  is approximately half that favored by chiral-perturbation theory. We constructed the IL3 to see if light nuclei are sensitive to this difference. In this model,  $A_{2\pi}^{PW}$  was fixed at a typical chiral-perturbation theory value and the cutoff parameter,  $c$ , and strengths  $A_R$  and  $A_{3\pi}^{\Delta R}$  were adjusted to fit the binding energies. The cutoff had to be made much softer to compensate for the strong  $A_{2\pi}^{PW}$ .

The expectation values of  $\delta v$  were calculated in a few nuclei for each model, and the values of  $A_R^*$  were estimated requiring:

$$\langle V_{ijk} - V_{ijk}^* \rangle \approx \langle \delta v(\mathbf{P}_{ij}) \rangle . \quad (3.39)$$

They are listed in Table I.

#### IV. QUANTUM MONTE CARLO CALCULATIONS

The GFMC calculations presented below were made using essentially the same methods and variational wave functions as described in Ref. [2] for our calculations of  $A \leq 8$  nuclei with the UIX three-nucleon potential. Here we describe only the few enhancements that were necessary for using the Illinois three-nucleon potentials.

The new terms in the Illinois potentials are static and hence present no formal difficulties for the GFMC propagator beyond those already encountered for the UIX  $V_{ijk}$ : they are included by expanding  $\exp(-\frac{1}{2}V_{ijk}\Delta\tau)$  to first order, as in Eq.(4.5) of Ref [2]. The structure of  $V^{2\pi, SW}$  is similar to that of the anticommutator part of  $V^{2\pi, PW}$  ( $V^{2\pi, A}$ ) and can also be reduced to just two-body operators in spin-isospin space. Thus it can be combined with the  $\alpha V_{ij;k}^{2\pi, A}$  in Eq.(4.21) of Ref [2] with almost no increase in the required computer time.

The  $V^{3\pi, \Delta R}$  involves many operators which are unfortunately not reducible to two-body operators in spin-isospin space, and thus, like  $V^{2\pi, C}$ , the commutator term of  $V^{2\pi, PW}$ , it adds a lot of time to the evaluation of a propagation step. In Ref [2], we showed that  $V^{2\pi, C}$  could be replaced with an increased strength of  $V^{2\pi, A}$  in the propagator with no loss of accuracy. The  $V^{3\pi, \Delta R}$  cannot be similarly completely replaced, but one can use two to four steps of

propagation with just an enhanced  $V^{2\pi,A}$  and then a correction; see Eq.(4.23) of Ref [2]. In general the tests we have made show that systematic errors in the GFMC calculations are less than 1% for the total energy; however  ${}^8\text{He}$  appears to be a particularly difficult case and the systematic errors for it are probably 2%.

The GFMC calculations for the models with  $V_{ijk}$  and p-shell nuclei were carried out as described in Ref. [2]. In particular, propagations were made to  $\tau = 0.2 \text{ MeV}^{-1}$  with steps of  $\Delta\tau = 0.0005 \text{ MeV}^{-1}$  (400 steps) and expectation values were computed every 20 steps with averages of the last 7 values ( $\tau \geq 0.14 \text{ MeV}^{-1}$ ) being used. The s-shell calculations for most models and some of the p-shell calculations for models without  $V_{ijk}$  were propagated to only  $\tau = 0.1 \text{ MeV}^{-1}$ . In most cases 10 unconstrained steps were used before each energy evaluation [ $n_u = 10$ ; see Eq.(4.17) of Ref. [2]], but 20 steps were used for some cases.

The  ${}^4\text{He}$  energy obtained with the Yakubovsky equations [30] and AV18/UIX Hamiltonian,  $-28.50(5) \text{ MeV}$ , is within  $\sim 0.5\%$  of the latest GFMC [2] result,  $-28.33(2) \text{ MeV}$ . The GFMC calculations are carried out with an approximation called AV8' [1], containing only the first 8 operators given in equations (2.4) and (2.5). The small difference between the AV18 and AV8' is treated perturbatively. It is therefore likely that the exact results for AV18/UIX are a little below the present GFMC results. The differences between GFMC and other calculations of binding energies of three and four nucleons will be the subject of another paper.

## V. RESULTS - LIGHT NUCLEI

This section presents various results for  $3 \leq A \leq 8$  nuclei and neutron drops using the new Illinois models, the AV18/UIX model, and Hamiltonians containing just the AV8' or AV18 potentials with no  $V_{ijk}$ . All of these results were obtained from GFMC calculations. With the exception of the total energy, which is discussed in the next paragraph, the values are perturbatively extrapolated from the mixed estimates, as described in Ref. [1]. Monte Carlo statistical errors are given in parentheses, but no estimate is made for the systematic errors associated with the extrapolation of mixed expectation values. The results presented in subsections A to F are with the simple  $H$  without boost interaction, whose contributions are reported in subsection G.

Most experimental energies and moments are drawn from the standard compilations of Ajzenberg-Selove [41] and the TUNL Nuclear Data Evaluation Project [42–44], while charge radii are taken from the NIKHEF compilation [45]. More recent data not included in these references are the energy of the  ${}^8\text{He}(2^+)$  state [46], the charge radius of  ${}^3\text{He}$  [47], and the  $A = 8$  magnetic and quadrupole moments [48].

### A. Energies of “Narrow” States

Table II shows our GFMC energies for  $3 \leq A \leq 8$  “narrow” states for all the Hamiltonians along with the corresponding experimental energies. The states are either particle stable, or have experimental widths less than 200 keV, and are used to fit the parameters of the Illinois models. The AV8' and AV18 Hamiltonians have no three-nucleon potential; they are



presented to show the importance of the  $V_{ijk}$ , and to provide results for comparison with those from other many-body methods.

The AV8' model consists of the Argonne  $v'_8$  two-nucleon potential, which is an eight-operator refit of the AV18, and the isoscalar Coulomb potential, as defined in Ref. [1]. The AV8' results should be the most reliable of all our results, because the GFMC propagation is made with the same Hamiltonian as is used for the energy expectation values, as discussed in Ref. [1]. In all other cases an effective  $H'$  is used for propagation and a small contribution  $\langle H - H' \rangle$  is evaluated perturbatively. In the cases that have a three-nucleon potential, the  $A_R$  is adjusted in  $H'$  to make  $\langle H - H' \rangle \sim 0$ ; however such an ability does not exist for the AV18 with no  $V_{ijk}$ . The AV18 energies are found by perturbatively evaluating  $\langle v_{18} - v'_8 \rangle$  in the AV8' calculation.

As described in the previous section, the AV18/IL1 and AV18/IL2 models differ only in the values of  $A_{2\pi}^{SW}$  and  $A_{2\pi}^{PW}$ , such that  $\langle V^{2\pi,SW} + V^{2\pi,PW} \rangle$  in IL2 is nearly the same as  $\langle V^{2\pi,PW} \rangle$  in IL1. We made a complete set of calculations for AV18/IL2 and perturbatively computed  $\langle V^{2\pi,PW} \rangle$  for AV18/IL1 in the AV18/IL2 wave functions. This result was used to generate 12 of the 21 AV18/IL1 energies in Table II. The procedure was checked by making a new propagation using the AV18/IL1  $H'$ , and these explicitly calculated values are shown for nine states; they are not significantly different from the perturbative estimates, i.e., the differences are generally smaller than the Monte Carlo errors.

The five Illinois Hamiltonians give very similar energies. The predictions for the p-shell nuclei are significantly better than those obtained with the AV18/UIX model. This is illustrated in Fig. 3 where results for the AV18/UIX, AV18/IL2, and AV18/IL4 models are compared to experiment. The relative stability of the helium and lithium nuclei with the Illinois models is clearly evident, as is the just unbound nature of  $^8\text{Be}$ . More quantitatively, Tables III and IV show various averages of the deviations from experiment for the narrow states of Table II. Table III is based on the deviations of the total energies of the 17 states, while Table IV is based on the deviations of the excitation energies of excited states. Both tables show the average deviation (which includes the signs of the deviations), the average of the magnitudes of the deviations, and the rms deviations. The average deviations in Table III demonstrate that the Hamiltonians with no  $V_{ijk}$  systematically underbind these nuclei by 5 to 7 MeV; AV18/UIX reduces this to the still large value of 2 MeV underbinding. The five Illinois models have no significant systematic under or overbinding. Because the errors for the AV8', AV18, and AV18/UIX cases are so one-sided, their average absolute and rms errors are comparable to their average signed errors. The rms error obtained with the AV18/IL1-5 Hamiltonians is  $\sim 1\%$ .

Table IV shows that the Hamiltonians with no  $V_{ijk}$  produce a spectrum that is too compressed, although it has far smaller deviations than the absolute energies. All of the Hamiltonians with  $V_{ijk}$  produce excitation spectra with significantly smaller rms deviations. However some of them (particularly AV18/IL2) are too expanded. The excitation spectra obtained with AV18/IL3 and AV18/IL4 appear to be somewhat better than the others.

## B. Contributions to the Energies

The contributions of the two-body potentials,  $v_{ij}$ , including electromagnetic terms, and the sum  $(K + v_{ij})$  are shown for several Hamiltonians in Table V. As was discussed in Ref. [1],

the perturbatively extrapolated values of  $\langle K \rangle$ ,  $\langle v_{ij} \rangle$ , and  $\langle V_{ijk} \rangle$  do not add up to the total energy,  $\langle H \rangle$ . The latter is the most reliably computed quantity. Other studies of GFMC calculations [49] suggest that the perturbative extrapolation of the potential energy is more reliable than that of the kinetic energy. Therefore the values of  $\langle K + v_{ij} \rangle$  are obtained by subtracting  $\langle V_{ijk} \rangle$  from  $\langle H \rangle$ ; estimates of  $\langle K \rangle$  may be obtained by subtracting  $\langle v_{ij} \rangle$  from  $\langle K + v_{ij} \rangle$ .

Table V shows some of the non-perturbative aspects of these calculations. For the p-shell nuclei, the total binding energy steadily increases from AV18 to AV18/UIX to the Illinois models. However the values of  $\langle K + v_{ij} \rangle$ , which involve the same operators in all cases, steadily decrease in magnitude. This is because the wave function is being tuned to the ever stronger  $V_{ijk}$  and hence is becoming less favorable for  $K + v_{ij}$ . The net increase in the binding energy comes from even bigger increases in  $\langle V_{ijk} \rangle$  (see Table VI). Although  $\langle K + v_{ij} \rangle$  is becoming less attractive in this progression,  $\langle v_{ij} \rangle$  is becoming more negative due to the enhanced tensor-isospin (pion-exchange) correlations induced in the wave function by  $V_{ijk}$ ; these correlations also increase the kinetic energy.

Table VI shows the total  $\langle V_{ijk} \rangle$  for the various models. The AV18/IL1 and AV18/IL2 models were constructed to have approximately the same  $\langle V_{ijk} \rangle$ . Although the AV18/IL3 model has very similar total binding energies as AV18/IL1 and AV18/IL2, there are significant differences in many of its contributions. This indicates that the correlations induced by IL3 (which is stronger and has a much softer pion form factor) in the wave functions make important non-perturbative changes in  $\langle K + v_{ij} \rangle$ . The AV18/IL4 and AV18/IL5 models have weaker strengths than the first three and smaller net  $\langle V_{ijk} \rangle$ . As expected, the  $\langle V_{ijk} \rangle$  for the Illinois models are all larger than for the AV18/UIX model in p-shell nuclei; they are also larger for the s-shell nuclei even though all the models give the same binding energies for these nuclei.

The fraction of the total binding energy represented by  $\langle V_{ijk} \rangle$  increases from s- to p-shell nuclei and as  $N - Z$  increases. For AV18/IL2 it is 17% for  ${}^3\text{H}$ , 30% for  ${}^4\text{He}$ , but then a nearly constant 33-37% for  ${}^6,7\text{Li}$  and  ${}^8\text{Be}$ . It then jumps to 49% for  ${}^8\text{Li}$  and 52% for  ${}^8\text{He}$ . Expressed as a fraction of the total potential energy, the AV18/IL2  $\langle V_{ijk} \rangle$  ranges from 2.5% for  ${}^3\text{H}$  to 6.1% for  ${}^4\text{He}$  up to 7.5% for  ${}^8\text{He}$ . These fractions are typical of the other Illinois models except that AV18/IL3 has somewhat larger ratios.

The individual contributions to  $\langle V_{ijk} \rangle$  are shown in Tables VII and VIII for AV18/IL2 and AV18/IL3, respectively. The ratios of the contributions of the anticommutator and commutator parts of  $V^{2\pi, PW}$  [see Eq.(3.3)] for the nuclei studied here are remarkably constant for a given model. For AV18/IL2 the ratio of the anticommutator contribution to the total  $\langle V^{2\pi, PW} \rangle$  varies only between 0.62 and 0.63 for the nuclei in Table VII, while it is 1.0 for pure neutron systems (the  $[\boldsymbol{\tau}_i \cdot \boldsymbol{\tau}_j, \boldsymbol{\tau}_j \cdot \boldsymbol{\tau}_k]$  is zero in  $T = \frac{3}{2}$  triples). Very similar ratios are obtained for AV18/UIX and the other Illinois models. A similar ratio has also been found in VMC calculations of  ${}^{16}\text{O}$  using an older Urbana model [50]. It is because of this very small variation that one cannot improve fits to the energies of light nuclei by changing the factor of  $\frac{1}{4}$  in Eq.(3.3).

The ratio of the contribution of  $V^{2\pi, SW}$  to that of  $V^{2\pi, PW}$  is also quite independent of nucleus. For AV18/IL2 it ranges from 3.6% for  ${}^8\text{He}$  to 4.2% for  ${}^3\text{H}$ . This ratio depends upon the model; for example, it is  $\sim 2.3\%$  for AV18/IL3 and  $\sim 5\%$  for AV18/IL4. Thus small changes in  $A_{2\pi}^{PW}$  can accurately compensate large changes in  $A_{2\pi}^{SW}$ , making it impossible to

uniquely determine the value of  $A_{2\pi}^{SW}$  from the binding energies of light nuclei. We have made versions of AV18/IL2 and AV18/IL3 that have the unreasonably large value of  $A_{2\pi}^{SW} = -2.2$  MeV; these also gave good fits to the binding energies of light nuclei.

The  $S_\tau^I S_\sigma^I$  and  $A_\tau^I A_\sigma^I$  terms of  $V^{3\pi, \Delta R}$  are shown in the columns labeled  $V^{3\pi, SS}$  and  $V^{3\pi, AA}$ , respectively. The  $S_\tau^I$  is a projector onto  $T = \frac{3}{2}$  triples and thus the  $S_\tau^I S_\sigma^I$  term of Eq.(3.31) vanishes in s-shell nuclei. The  $A_\tau^I A_\sigma^I$  term results in a repulsive contribution in nuclei and hence  $V^{3\pi, \Delta R}$  is repulsive in s-shell nuclei. In p-shell nuclei the  $S_\tau^I S_\sigma^I$  term of  $V^{3\pi, \Delta R}$  is attractive and larger in magnitude than the  $A_\tau^I A_\sigma^I$  term. Thus the  $V^{3\pi, \Delta R}$  changes sign between s-shell and p-shell nuclei and also becomes more attractive as  $N - Z$  increases. This allows  $V^{3\pi, \Delta R}$  to substantially improve the fit to the energies of light nuclei. Its strength is therefore rather well determined by the data in the context of present models. In low-density neutron drops the  $V^{2\pi}$  terms become very small, while the  $V^{3\pi, \Delta R}$  is attractive and gives the largest contribution to  $V_{ijk}$ .

An interesting property of the  $A_\tau^I A_\sigma^I$  term is that it only increases by a factor of  $\sim 3$  as  $A$  increases from 3 to 4, while all the other  $V_{ijk}$  terms rise by a factor of 5.5. The factor of 5.5 can be understood from the simple argument that  ${}^4\text{He}$  has four triples compared to only one triple in the trinucleons, and each triple in  ${}^4\text{He}$  gives  $\sim 40\%$  more contribution due to the higher density from increased binding. The  $V^{2\pi}$  and  $V^R$  have relatively simple spatial dependence given by a product two radial functions; in contrast the  $A_\sigma^I$  has a more complex spatial dependence, given by Eq.(A6), containing radial functions of all the three pair distances. In principle, the strength of the  $A_\tau^I A_\sigma^I$  term in  $V_{ijk}$  can be adjusted separately from the  $S_\tau^I S_\sigma^I$  term to reproduce the energies of  ${}^4\text{He}$  and the trinucleons with the desired precision; however, agreement with less than 1% error can be obtained assuming that the strengths of the  $S_\tau^I S_\sigma^I$  and  $A_\tau^I A_\sigma^I$  terms of  $V^{3\pi, \Delta R}$  have the theoretical ratio of 50/26 from Eq.(3.31).

Table IX shows the  $v^\pi$ ,  $V^{2\pi}$ ,  $V^{3\pi, \Delta R}$ , and the remainder contributions to the potential-energy expectation values, evaluated for AV18/IL2. Note that additional pion-exchange contributions omitted from  $v^\pi$ ,  $V^{2\pi}$  and  $V^{3\pi, \Delta R}$  are contained in the  $v^R$  and  $V^R$ . For example, the two-pion-exchange two-nucleon interaction provides most of the intermediate-range part of  $v^R$ . The total two-pion terms of  $V_{ijk}$  are typically 11% of the one-pion part of  $v_{ij}$  for the AV18/UIX, AV18/IL4, and AV18/IL5 models, while they are 16% for AV18/IL2 and 21% for AV18/IL3. The ratio of  $V^{3\pi, \Delta R}$  to  $V^{2\pi}$  changes sign between s-shell and p-shell nuclei.

The ratio of the  $V^{2\pi}$  and  $V^R$  contributions for a given model does not change by much in the light nuclei. For the AV18/IL2 model, the ratio is  $-2.23$  for s-shell nuclei and  $-1.97$  for  ${}^8\text{Li}$ . The AV18/IL4 model has the largest range, from  $-2.8$  for s-shell nuclei to  $-2.35$  for  ${}^8\text{Li}$ . When only  ${}^3\text{H}$  and  ${}^4\text{He}$  are included in the fit, as in the case of the UIX model, it is not possible to determine  $A_{2\pi}^{PW}$  and  $A_R$  separately. For this reason the equilibrium density of nuclear matter was used in Ref. [1] to determine  $A_R$  even though exact calculations of nuclear matter properties are not yet possible.

Even after including all  $A \leq 8$  nuclei in the fit, we cannot determine  $A_{2\pi}^{PW}$ ,  $A_R$  and  $A_{3\pi}^{\Delta R}$  separately. For example, in AV18/IL2, decreasing  $A_R$  and  $A_{2\pi}^{PW}$  by factors of 0.5 and 0.77 leaves the energies of  ${}^3\text{H}$  and  ${}^4\text{He}$  unchanged in first order, however, that of  ${}^8\text{Li}$  decreases by 0.8 MeV, *i.e.* by  $\sim 2\%$ . This change can be compensated by reducing  $A_{3\pi}^{\Delta R}$  by  $\sim 20\%$ . Thus in first order multiplying  $A_R$ ,  $A_{2\pi}^{PW}$  and  $A_{3\pi}^{\Delta R}$  by 0.5, 0.77 and 0.8 leave the energies of s-shell nuclei and  ${}^8\text{Li}$  unchanged.

The strengths of  $A_R$ ,  $A_{2\pi}^{PW}$  and  $A_{3\pi}^{\Delta R}$  in IL4 are respectively 0.55, 0.76 and 0.81 times those in IL2. The difference between these ratios and those in the preceding paragraph is due to nonperturbative effects. The overall fit obtained with IL4 is slightly better than that with IL2 (see Tables III and IV), especially for excitation energies, suggesting that the parameters of IL4 have more realistic values. Preliminary results obtained for  $A = 9, 10$  nuclei also indicate that IL4 is better than IL2.

### C. Isobaric Analog Energies

Table X gives the total isovector ( $n = 1$ ) and isotensor ( $n = 2$ ) energy coefficients,  $a_{A,T}^{(n)}$ , defined in Eq.(5.3) of Ref. [2], for energy differences in isobaric multiplets. The first three lines of the table show three different evaluations of the  $a_{3,\frac{1}{2}}^1$ . The first two are expectation values of the isovector operators in separately computed  ${}^3\text{H}$  and  ${}^3\text{He}$  GFMC wave functions, respectively. The last is the difference of separately computed GFMC energies; it has a considerably larger statistical error, but otherwise would be the best calculation to compare to experiment. The expectation values computed in the two different wave functions are statistically different, but, due to its larger error, the energy difference is consistent with both.

The  $a_{A,T}^{(n)}$  in multiplets having  $A > 3$  (Table X) have been computed as expectation values of the isovector and isotensor parts of the Hamiltonians in the wave function for the  $Z = \frac{1}{2}A - T$  nucleus. Table XI gives a breakdown of these coefficients into various contributions for the AV18/IL2 model. These include:  $K^{CSB}$ , the kinetic energy contribution due to the neutron-proton mass difference;  $v_{C1}(pp)$ , the proton-proton Coulomb term;  $v^{\gamma,R}$ , the remaining electromagnetic contributions, such as magnetic moment interactions, which are part of Argonne  $v_{18}$ ; and the strong-interaction terms  $v^{CSB}$  and  $v^{CD}$ . The isotensor  $v^{CD}$  comes from components 15–17 of Argonne  $v_{18}$  and contributes only to the  $a^{(2)}$ , while the isovector  $v^{CSB}$  is term 18 and contributes only to  $a^{(1)}$ .

The isovector terms are dominated by  $v_{C1}(pp)$ , the expectation value of which is strongly correlated with the rms radii. The Illinois models generally give better total binding energies and radii (see below) and thus better values for these coefficients. However, the remaining kinetic and potential terms contribute 5–10% of the total isovector energy coefficient, thus playing an important part in the overall good agreement with experiment. The isotensor terms are also dominated by  $v_{C1}(pp)$ , but in this case the increased binding of the Illinois models has not improved the agreement with experiment. The  $v_{C1}(pp)$  alone underestimates the  $a_{A,T}^{(2)}$ ; the strong interaction contributions have the correct sign, but seem to be too large in magnitude.

### D. Energies of “Wide” States and Spin-orbit Splittings

So far we have presented results for states of nuclei that are either particle stable or have narrow experimental widths. Our GFMC calculations which treat all states as bound systems should be reliable for such states, and the comparison of the resulting energies to experimental values should be unambiguous. Table XII shows GFMC calculations of additional states that are experimentally broad or experimentally unknown. An example

of the GFMC propagation for broad and narrow states was shown in [2]; the energy of the broad state falls slowly but steadily with imaginary time. This introduces a certain, but usually small, ambiguity in determining the resonance energy from the calculation; we use the average of the the energies for  $0.14 \leq \tau \leq 0.20 \text{ MeV}^{-1}$ . In addition, the experimental assignment of some resonance energies may be difficult. Nonetheless, the rms errors in the Illinois predictions of the experimentally known states in Table XII are only  $\sim 700 \text{ keV}$ .

It has long been known that Hamiltonians containing only realistic two-nucleon potentials often cannot correctly predict the observed spin-orbit splitting of nuclear levels; in fact one of the original motivations for the Fujita-Miyazawa three-nucleon potential was the study of spin-orbit splittings [11]. In [51] we showed that one of the Urbana family of  $V_{ijk}$  makes a substantial contribution to the spin-orbit splitting in  $^{15}\text{N}$ . Table XIII shows calculated and experimental splittings for a number of states that are spin-orbit partners in conventional shell-model calculations. The dominant  $L$  and  $S$  in the shell-model calculations (and in the one-body parts of our variational wave functions) are shown.

The spin-orbit splitting computed with just the two-nucleon interactions, AV8' or AV18 are generally too small, sometimes by factors of two to three. In some cases AV18/UIX makes a significant increase, but in general it also predicts too small splittings. The predictions with the Illinois models are in much better agreement with the experimental values. Due to significant statistical errors in the calculated spin-orbit splittings and the fact that some of the spin-orbit partners are wide states, they cannot yet be used to differentiate between the various Illinois models.

### E. Point Nucleon Radii and Electromagnetic Moments

Table XIV gives the point proton and neutron radii for some of these models. The “experimental” point proton radii were obtained by subtracting a proton mean-square radius of  $0.743 \text{ fm}^2$  and  $\frac{N}{Z}$  times a neutron mean-square radius of  $-0.116 \text{ fm}^2$  from the squares of the measured charge radii. As mentioned earlier the GFMC propagations are carried out for an  $H'$ , and results for the desired  $H$  are obtained by treating  $H - H'$  as a first order perturbation. Therefore the point radii and electromagnetic moments are computed for  $H'$  instead of  $H$ . For the models with three-body potentials, the  $H'$  has a modified  $A_R$  such that  $\langle H - H' \rangle \sim 0$ , and thus the radii and moments for the  $H'$  should be close to the desired ones for  $H$ . However the calculations for AV18 with no three-body potential use just AV8' for  $H'$ . In this case  $\langle H - H' \rangle$  is significantly different from zero, and we can only quote radii and moments for AV8'. For the few light p-shell nuclei that have measured radii, those obtained with the Illinois models, which produce good binding energies, are in better agreement with the data than those obtained with either AV8' or AV18/UIX.

Table XV shows the experimental isoscalar and isovector magnetic moments for the cases that have been measured along with values calculated using only one-body current operators. The values in the table are defined in the same way as the coefficients  $a_{A,T}^{(n)}$  in Table X (see Eq.(5.3) of Ref. [2]) and thus the isovector ( $\mu^{(1)}$ ) values for  $T = \frac{1}{2}$  cases are  $-2$  times those often quoted. The  $\mu^{(0)}$  and  $\mu^{(1)}$  are obtained from expectation values of the isoscalar and isovector magnetic-moment operators in the wave function for the nucleus having smallest  $Z = \frac{1}{2}A - T$ . In this approximation the isotensor  $\mu^{(2)} = 0$ , since the one-body magnetic-moment operator does not have an isotensor term. However, one may obtain a small  $\mu^{(2)}$

when the magnetic moments are separately calculated for each state in the multiplet due to violation of isospin symmetry in the wave functions.

For the  $A = 8$ ,  $T = 1$  nuclei, the experimental isoscalar and isovector moments are obtained from the sum and difference of the values for B and Li, since the magnetic moment of the  $T = 1$   $J^\pi = 2^+$  state in Be is not measured. In fact the sum gives  $2\mu^{(0)} + \mu^{(2)}$ , but in the present approximation  $\mu^{(2)} = 0$ .

The computed magnetic moments show little dependence on the three-nucleon interaction. Because pair currents are not included in the calculated values in Table XV, one cannot expect good agreement with the experimental values, especially for the isovector values. The pair-current corrections computed for the  $A = 3$  system using the AV18/UIX model are 0.034 and  $-0.778$  for the isoscalar and isovector moments, respectively [52]. This isoscalar correction is twice what is needed to achieve agreement with experiment while the isovector value results in perfect agreement. All the computed magnetic moments differ from the experimental values by amounts comparable to the corrections computed for  $A = 3$ .

Table XVI shows computed (again using just impulse approximation) and experimental quadrupole moments. The Illinois models predict quadrupole moments that are generally smaller than those obtained using AV18/UIX. This is a consequence of the increased binding energy, and resulting smaller rms radii. The situation for  ${}^6\text{Li}$  is very difficult due to the large cancellation between orbital and intrinsic components (in an alpha-deuteron picture) of the quadrupole moment.

## F. Neutron Drops

Neutron drops are systems of interacting neutrons confined in an artificial external well. We have previously reported results for systems of seven and eight neutrons as a basis for comparing Skyrme models of neutron-rich systems with microscopic calculations based on realistic interactions [18]. The determination of the isospin dependence of the Skyrme model spin-orbit parameters is of particular interest. The external one-body well that we use is a Woods-Saxon:

$$V_1(r) = \sum_i \frac{V_0}{1 + \exp[-(r_i - r_0)/a_0]} ; \quad (5.1)$$

the parameters are  $V_0 = -20$  MeV,  $r_0 = 3.0$  fm, and  $a_0 = 0.65$  fm. Neither the external well nor the total internal potential ( $v_{ij} + V_{ijk}$ ) are individually attractive enough to produce bound states of seven or eight neutrons; however the combination does produce binding.

Many of the tables show results for the neutron drops. The  $T = \frac{3}{2}$  nature of the  $S_\tau^I S_\sigma^I$  term of  $V^{3\pi, \Delta R}$  results in large contributions in the neutron drops. As a result the seven-neutron drops computed with some of the Illinois potentials have double the spin-orbit splitting predicted by AV18/UIX. This strong dependence on the Hamiltonian indicates that the conclusion of [18], that conventional Skyrme models over-predict the spin-orbit splitting in neutron-rich systems may not be valid. The IL3 model gives larger spin-orbit splitting in the  $A = 7$  neutron drop than the others.

## G. $\delta v$ Contributions

Table XVII shows the expectation values of  $\delta v$  in various nuclei for some of the Illinois Hamiltonians along with the net change in the binding energy due to the boost correction:

$$\langle H^* - H \rangle = \langle \delta v + (V_{ijk}^* - V_{ijk}) \rangle . \quad (5.2)$$

In the light nuclei the net change is, at most, comparable to 1% of the binding energies, and therefore the Hamiltonian  $H^*$  [Eq.(3.35)] gives essentially the same energies as the simpler  $H$  [Eq.(2.1)] without  $\delta v$  correction. However, the net change is not necessarily small in other nuclear systems like nuclear or neutron matter or neutron drops. In the  $A = 8$  drop (Table XVII) the  $\langle V_{ijk} - V_{ijk}^* \rangle$  is only half as large as  $\langle \delta v \rangle$ . In these systems we must use the Hamiltonian  $H^*$ .

## VI. CONCLUSIONS AND DISCUSSION

We find that nonrelativistic Hamiltonians containing two- and three-nucleon interactions can reproduce the energies of all the bound and narrow states of up to eight nucleons with an rms error  $\lesssim 1\%$  via GFMC calculations, which have an estimated error of  $< 2\%$ . The three-nucleon interactions give a significant fraction of nuclear binding energy due to a large cancellation between the kinetic and two-nucleon interaction energies. This cancellation is seen even in the deuteron whose kinetic and interaction energies obtained from AV18 are respectively +19.9 and  $-22.1$  MeV. Since the AV18 model is very successful in explaining the observed deuteron form factors, and all realistic models of  $v_{ij}$  also have this feature, it seems to be inherent in nuclei.

The Bochum group [53] obtained a one parameter family of  $V_{ijk}$  models by choosing the cutoff mass in the TM model of  $V^{2\pi}$ , including P- and S-wave terms, to reproduce the  ${}^3\text{H}$  or  ${}^3\text{He}$  energy with several modern  $v_{ij}$ . More recently [30] they have obtained results for  ${}^3\text{H}$ ,  ${}^3\text{He}$  and  ${}^4\text{He}$  with AV18 and a revised version of TM  $V^{2\pi}$  as well as the UIX model. They observe that when the energy of  ${}^3\text{He}$  is reproduced that of  ${}^4\text{He}$  is very close to the observed, but  ${}^3\text{H}$  is underbound by  $\sim 0.5\%$ . On the other hand if  ${}^3\text{H}$  energy is reproduced both  ${}^3\text{He}$  and  ${}^4\text{He}$  are overbound by less than 1%. In order to improve the accuracy of nuclear Hamiltonians beyond 99%, a more quantitative description of the charge symmetry breaking interactions is necessary.

The above results limit the contribution of four-nucleon interactions in  ${}^4\text{He}$  to less than 1% of its binding energy. The  $\langle V_{ijk} \rangle$  contributes approximately a quarter of the  ${}^4\text{He}$  binding, although the difference of the total energies computed with and without a  $V_{ijk}$  is only a seventh of the binding energy. The ratio of the expectation values of  $V_{ijk}$  and  $v_{ij}$  is  $\sim 7\%$  in the  $A = 8$  nuclei, and  $\langle V_{ijk} \rangle$  gives up to one half of their binding energy. If the four-nucleon interactions were to contribute  $\sim 6\%$  of  $V_{ijk}$ , they could influence the  $A = 8$  binding energies by  $\sim 3\%$ . The present calculations do not indicate a need to include four-nucleon interactions to fit the observed energies at the 1% level. Thus, either the four-nucleon contributions are smaller than 1% of the binding energies, or parts of the present models of  $V_{ijk}$  are mocking up their effects.

The energies of light nuclei can be used to determine at most three parameters of  $V_{ijk}$ . We can choose them as either the strengths  $A_{2\pi}^{PW}$ ,  $A_{3\pi}^{\Delta R}$  and  $A_R$ , or use a theoretical value

of  $A_{2\pi}^{PW}$  and fit the short-range cutoff. It is possible to make correlated changes in the three strengths, as in models IL2 and IL4, which have relatively small effect on the energies of light nuclei.

All the realistic models of  $V_{ijk}$ , including the older Urbana models, have a cancellation between the attractive  $V^{2\pi}$  and repulsive  $V^R$ . For example, their contributions in the AV18/IL2 model, to the energy of  ${}^3\text{He}$  ( ${}^8\text{Be}$ ) are respectively  $-2.8$  ( $-37$ ) and  $1.3$  ( $18$ ) MeV. The contribution of  $V^R$  grows faster than that of  $V^{2\pi}$  as either  $A$  or the density of matter increases, and lowers the saturation density of symmetric nuclear matter. It is difficult to determine the  $A_R$  quantitatively from the energies of light nuclei.

Such a cancellation was noticed in Faddeev calculations including  $\Delta$  components in the triton wave function [35,36]. The estimates of Picklesimer, Rice and Brandenburg [36] indicated that the  $\Delta$  part of  $V^{2\pi, PW}$  changes the  ${}^3\text{H}$  energy by only  $\sim -0.75$  MeV, while the processes, which represent the suppression of the attractive two-nucleon  $v^{2\pi}$  by the third nucleon via the dispersion effect, give  $\sim 1.1$  MeV. The  $V^R$  contribution in present models is comparable to their  $\Delta$  dispersive effect, while the  $V^{2\pi, PW}$  is much more attractive.

Studies of  $A = 3, 4$  nuclei with relativistic Hamiltonians [17] indicate that the boost interaction  $\delta v$  gives the largest relativistic correction, of  $\sim 0.4$  MeV, to the triton energy. It is included in the present relativistic ( $H^*$ ) models. The other corrections included in the relativistic Hamiltonians, but excluded here, are only  $\sim 0.1 \pm 0.05$  MeV, *i.e.* of order 1%. However, three-nucleon interactions via Z-diagrams [54], if any, have to be added to the  $V_{ijk}^*$  in the relativistic Hamiltonians. Forest [55] has estimated their contribution to the triton, using the scalar and vector parts of AV18  $v_{ij}$ , obtained with Riska's method, to be  $\sim 0.3$  MeV. In the present Illinois models these are also buried in the  $V^{R*}$ . In the initial Illinois models discussed at the International Nuclear Physics Conference in Paris [56] we attempted to include possible Z-diagram contributions in  $V_{ijk}$ , however, the observed energies can be reproduced without them. If these exist, then, as in the case of  $V^{2\pi, SW}$ , we can assume theoretical values for their strengths and fit the energies, presumably with  $\sim 1\%$  accuracy, by readjusting the strengths  $A_{2\pi}^{PW}$ ,  $A_{3\pi}^{\Delta R}$  and  $A_R^*$ . Nuclear binding energies seem to require only three components in the  $V_{ijk}^*$ , an attractive part to provide more binding to light nuclei, a repulsive part to make nuclear matter  $E(\rho)$  saturate at empirical  $\rho_0$ , and an isospin-dependent term to provide extra binding to the neutron-rich helium isotopes.

Preliminary versions of the IL1-IL3 models were also discussed at the Few-Body Physics conference in Taipei [57]. The parameters of the Illinois models reported there were incorrect due to a programming error. The correct values are as reported here. Since then the IL3 model has been revised. In the present IL3 model, softer cutoffs are used also in the  $V^R$  terms. Results for nuclear and neutron matter with the Illinois models will be published separately.

As mentioned in the introduction, additional data necessary to further the study of  $V_{ijk}$  may be obtained from the scattering of nucleons by deuterium. It is known that most of the low energy  $Nd$  elastic scattering observables are well reproduced by realistic models of  $v_{ij}$  [27]. The expectation value of  $V_{ijk}$  is only  $\sim 2.5\%$  of that of  $v_{ij} + v_{jk} + v_{ki}$  in  ${}^3\text{H}$ , thus it is not expected to have a large effect on this scattering. However, all realistic models of  $v_{ij}$  underestimate the observed nucleon analyzing power  $A_y$  in low energy  $Nd$  scattering; the spin-orbit splitting induced by the  $V^{2\pi, PW}$  of the various  $V_{ijk}$  reduces the error somewhat but the additional spin-orbit splitting induced by the present Illinois models is probably



inadequate to completely correct the underestimate [58].

More recently it has also been suggested that minima and polarization observables of  $Nd$  elastic scattering at intermediate energies are sensitive to  $V_{ijk}$ , and may be used to refine models of  $V_{ijk}$  [59–61]. Thus further improvements in realistic models of  $V_{ijk}$  may be possible by a simultaneous fit to  $Nd$  scattering observables and nuclear binding energies. Since  $Nd$  scattering is sensitive only to the  $V_{ijk}$  in the total isospin  $T = 1/2$  state, it does not provide information on the  $V_{ijk}$  in the  $T = 3/2$  state. This work shows the need for an attractive interaction in  $T = 3/2$  states to reproduce the energies of  $p$ -shell nuclei. It may be possible to access this part of  $V_{ijk}$  in  $n - t$  and  $p - {}^3\text{He}$  scattering.

### ACKNOWLEDGMENTS

The many-body calculations were made possible by generous grants of time on the parallel computers of the Mathematics and Computer Science Division, Argonne National Laboratory, and by early-user time on the IBM SP at the National Energy Research Scientific Computing Center. The work of SCP and RBW is supported by the U.S. Department of Energy, Nuclear Physics Division, under contract No. W-31-109-ENG-38, that of VRP by the U.S. National Science Foundation via grant PHY 98-00978, and that of JC by the U.S. Department of Energy under contract W-7405-ENG-36.

### APPENDIX: THE SPIN-SPACE OPERATORS IN $V^{3\pi, \Delta R}$

It is convenient to define the functions:

$$t_{ij} = \frac{3T(m_\pi r_{ij})}{r_{ij}^2}, \quad (\text{A1})$$

$$y_{ij} = Y(m_\pi r_{ij}) - T(m_\pi r_{ij}), \quad (\text{A2})$$

with which the spin-space operator  $X_{ij}$  in  $v_{ij}^\pi$  [Eq.(3.7)] can be expressed as:

$$X_{ij} = t_{ij} \boldsymbol{\sigma}_i \cdot \mathbf{r}_{ij} \boldsymbol{\sigma}_j \cdot \mathbf{r}_{ij} + y_{ij} \boldsymbol{\sigma}_i \cdot \boldsymbol{\sigma}_j. \quad (\text{A3})$$

Evaluating the  $\Delta$ -ring diagrams using closure approximation then gives:

$$\begin{aligned} S_\sigma^I &= 2y_{ij}y_{jk}y_{ki} + \frac{2}{3} \sum_{cyc} (r_{ij}^2 t_{ij} y_{jk} y_{ki} + C_j^2 t_{ij} t_{jk} y_{ki}) - \frac{2}{3} C_i C_j C_k t_{ij} t_{jk} t_{ki} \\ &+ \left[ \sum_{cyc} \boldsymbol{\sigma}_i \cdot \boldsymbol{\sigma}_j \right] \left[ \frac{2}{3} y_{ij} y_{jk} y_{ki} + \frac{1}{3} \sum_{cyc} r_{ij}^2 t_{ij} y_{jk} y_{ki} \right] + \frac{1}{3} \sum_{cyc} \boldsymbol{\sigma}_i \cdot \boldsymbol{\sigma}_k C_j^2 t_{ij} t_{jk} y_{ki} \\ &- \frac{1}{3} \sum_{cyc} (\boldsymbol{\sigma}_i \cdot \mathbf{r}_{ij} \boldsymbol{\sigma}_j \cdot \mathbf{r}_{ij} t_{ij} y_{ki} y_{jk} + \boldsymbol{\sigma}_i \cdot \mathbf{r}_{ki} \boldsymbol{\sigma}_j \cdot \mathbf{r}_{ki} t_{ki} y_{jk} y_{ij} + \boldsymbol{\sigma}_i \cdot \mathbf{r}_{jk} \boldsymbol{\sigma}_j \cdot \mathbf{r}_{jk} t_{jk} y_{ij} y_{ki}) \\ &+ \frac{1}{3} \sum_{cyc} C_k \boldsymbol{\sigma}_i \cdot \mathbf{r}_{jk} \boldsymbol{\sigma}_j \cdot \mathbf{r}_{ki} t_{ki} t_{jk} y_{ij} \\ &+ \frac{1}{3} \sum_{cyc} \boldsymbol{\sigma}_i \cdot \mathbf{a} \boldsymbol{\sigma}_j \cdot \mathbf{a} (t_{ij} t_{jk} y_{ki} + t_{ij} y_{jk} t_{ki} + C_k t_{ij} t_{jk} t_{ki}), \end{aligned} \quad (\text{A4})$$

$$\begin{aligned}
S_{\sigma,ijk}^D &= \frac{1}{3} \boldsymbol{\sigma}_j \cdot \boldsymbol{\sigma}_k \left[ 2y_{ij}y_{jk}y_{ki} + C_i^2 t_{ij}y_{jk}t_{ki} + r_{ij}^2 t_{ij}y_{ki}y_{jk} + r_{jk}^2 t_{jk}y_{ij}y_{ki} + r_{ki}^2 t_{ki}y_{jk}y_{ij} \right] \\
&+ \frac{1}{3} C_i \boldsymbol{\sigma}_j \cdot \mathbf{r}_{ki} \boldsymbol{\sigma}_k \cdot \mathbf{r}_{ij} t_{ij}y_{jk}t_{ki} - \frac{1}{3} \boldsymbol{\sigma}_j \cdot \mathbf{r}_{ij} \boldsymbol{\sigma}_k \cdot \mathbf{r}_{ij} t_{ij}y_{ki}y_{jk} \\
&- \frac{1}{3} \boldsymbol{\sigma}_j \cdot \mathbf{r}_{ki} \boldsymbol{\sigma}_k \cdot \mathbf{r}_{ki} t_{ki}y_{jk}y_{ij} - \frac{1}{3} \boldsymbol{\sigma}_j \cdot \mathbf{r}_{jk} \boldsymbol{\sigma}_k \cdot \mathbf{r}_{jk} t_{jk}y_{ij}y_{ki} \\
&+ \frac{1}{3} \boldsymbol{\sigma}_j \cdot \mathbf{a} \boldsymbol{\sigma}_k \cdot \mathbf{a} (t_{ij}t_{jk}y_{ki} + y_{ij}t_{jk}t_{ki} + C_i t_{ij}t_{jk}t_{ki}) , \tag{A5}
\end{aligned}$$

$$\begin{aligned}
A_{\sigma}^I &= \frac{i}{3} [\boldsymbol{\sigma}_i \cdot \boldsymbol{\sigma}_j \times \boldsymbol{\sigma}_k y_{ij}y_{jk}y_{ki} + \boldsymbol{\sigma}_i \cdot \mathbf{a} \boldsymbol{\sigma}_j \cdot \mathbf{a} \boldsymbol{\sigma}_k \cdot \mathbf{a} t_{ij}t_{jk}t_{ki}] \\
&+ \frac{i}{3} \sum_{cyc} (\boldsymbol{\sigma}_i \times \boldsymbol{\sigma}_j \cdot \mathbf{r}_{ij} \boldsymbol{\sigma}_k \cdot \mathbf{r}_{ij} t_{ij}y_{jk}y_{ki} + \boldsymbol{\sigma}_i \cdot \mathbf{a} \boldsymbol{\sigma}_j \cdot \boldsymbol{\sigma}_k C_i t_{ij}y_{jk}t_{ki}) \\
&+ \frac{i}{3} \sum_{cyc} \boldsymbol{\sigma}_i \cdot \mathbf{r}_{jk} \boldsymbol{\sigma}_k \cdot \mathbf{r}_{ij} \boldsymbol{\sigma}_j \cdot \mathbf{a} t_{ij}t_{jk}y_{ki} \\
&+ \frac{2i}{3} \sum_{cyc} \boldsymbol{\sigma}_i \cdot \mathbf{a} (C_i t_{ij}y_{jk}t_{ki} - C_j t_{ij}t_{jk}y_{ki} - C_k y_{ij}t_{jk}t_{ki} - C_j C_k t_{ij}t_{jk}t_{ki}) , \tag{A6}
\end{aligned}$$

and

$$A_{\sigma,ijk}^D = -\frac{i}{3} \boldsymbol{\sigma}_i \cdot \mathbf{a} (C_i t_{ij}y_{jk}t_{ki} - C_j t_{ij}t_{jk}y_{ki} - C_k y_{ij}t_{jk}t_{ki} - C_j C_k t_{ij}t_{jk}t_{ki}) . \tag{A7}$$

The  $C_i = \mathbf{r}_{ij} \cdot \mathbf{r}_{ik}$  and  $\mathbf{a} = \mathbf{r}_{ij} \times \mathbf{r}_{jk}$ . A cyclic sum over the indices  $ijk$  is denoted by *cyc*.

## REFERENCES

- \* Electronic address: spieper@anl.gov
  - † Electronic address: vijay@rsm1.physics.uiuc.edu
  - ¶ Electronic address: wiringa@anl.gov
  - ‡ Electronic address: carlson@paths.lanl.gov
- [1] B. S. Pudliner, V. R. Pandharipande, J. Carlson, S. C. Pieper, and R. B. Wiringa, Phys. Rev. C **56**, 1720 (1997).
  - [2] R. B. Wiringa, S. C. Pieper, J. Carlson, and V. R. Pandharipande, Phys. Rev. C **62**, 014001 (2000).
  - [3] A. Akmal, V. R. Pandharipande, and D. G. Ravenhall, Phys. Rev. C **58**, 1804 (1998).
  - [4] R. B. Wiringa, V. G. J. Stoks, and R. Schiavilla, Phys. Rev. C **51**, 38 (1995).
  - [5] B. S. Pudliner, V. R. Pandharipande, J. Carlson, and R. B. Wiringa, Phys. Rev. Lett. **74**, 4396 (1995).
  - [6] V. G. J. Stoks, R. A. M. Klomp, M. C. M. Rentmeester, and J. J. de Swart, Phys. Rev. C **48**, 792 (1993).
  - [7] A. Kievsky, M. H. Wood, C. R. Brune, B. M. Fisher, H. J. Karwowski, D. S. Leonard, E. J. Ludwig, S. Rosati, and M. Viviani, Phys. Rev. C **63**, 024005 (2001).
  - [8] H. Wiatała, W. Glöckle, J. Golak, A. Nogga, H. Kamada, R. Skibiński, and J. Kuroś-Żolnierczuk, Phys. Rev. C **63**, 024007 (2001).
  - [9] S. A. Coon and J. L. Friar, Phys. Rev. C **34**, 1060 (1986).
  - [10] H. Primakoff and T. Holstein, Phys. Rev. **38**, 1218 (1939).
  - [11] J. Fujita and H. Miyazawa, Prog. Theor. Phys. **17**, 360 (1957); **17**, 366 (1957).
  - [12] S. A. Coon, M. D. Scadron, P. C. McNamee, B. R. Barrett, D. W. E. Blatt, and B. H. J. McKellar, Nucl. Phys. **A317**, 242 (1979).
  - [13] H. T. Coelho, T. K. Das, and M. R. Robilotta, Phys. Rev. C **28**, 1812 (1983).
  - [14] J. L. Friar, D. Hüber, and U. van Kolck, Phys. Rev. C **59**, 53 (1999).
  - [15] J. Carlson, V. R. Pandharipande, and R. B. Wiringa, Nucl. Phys. **A401**, 59 (1983).
  - [16] J. Carlson, V. R. Pandharipande, and R. Schiavilla, Phys. Rev. C **47**, 484 (1993).
  - [17] J. L. Forest, V. R. Pandharipande, and A. Arriaga, Phys. Rev. C **60**, 014002 (1999).
  - [18] B. S. Pudliner, A. Smerzi, J. Carlson, V. R. Pandharipande, S. C. Pieper, and D. G. Ravenhall, Phys. Rev. Lett. **76**, 2416 (1996).
  - [19] M. Lacombe, B. Loiseau, J. M. Richard, R. Vinh Mau, J. Côté, P. Pirès, and R. de Tournreil, Phys. Rev. C **21**, 861 (1980).
  - [20] V. G. J. Stoks, R. A. M. Klomp, C. P. F. Terheggen, and J. J. de Swart, Phys. Rev. C **49**, 2950 (1994).
  - [21] R. Machleidt, F. Sammarruca, and Y. Song, Phys. Rev. C **53**, R1483 (1996).
  - [22] R. Schiavilla *et al.*, Phys. Rev. C **58**, 1263 (1998).
  - [23] L. C. Alexa *et al.*, Phys. Rev. Lett. **82**, 1374 (1999).
  - [24] D. Abbott *et al.*, Phys. Rev. Lett. **82**, 1383 (1999).
  - [25] D. Abbott *et al.*, Phys. Rev. Lett. **84**, 5053 (2000).
  - [26] Z.-L. Zhou *et al.*, Phys. Rev. Lett. **82**, 687 (1999).
  - [27] J. Carlson and R. Schiavilla, Rev. Mod. Phys. **70**, 743 (1998).
  - [28] J. L. Forest, Phys. Rev. C **61**, 034007 (2000).
  - [29] J. L. Friar, G. L. Payne, V. G. J. Stoks, and J. J. de Swart, Phys. Lett. B **311**, 4 (1993).
  - [30] A. Nogga, H. Kamada, and W. Glöckle, Phys. Rev. Lett. **85**, 944 (2000).

- [31] L. Engvik, M. Hjorth-Jensen, R. Machleidt, H. Mütter, and A. Polls, Nucl. Phys. **A627**, 85 (1997); L. Engvik, Thesis, University of Oslo (1999).
- [32] J. L. Friar, Phys. Rev. C **60**, 034002 (1999).
- [33] J. L. Forest, V. R. Pandharipande, and J. L. Friar, Phys. Rev. C **52**, 568 (1995).
- [34] J. L. Friar, Phys. Rev. C **12**, 695 (1975).
- [35] Ch. Hadjuk, P. U. Sauer, and S. N. Yang, Nucl. Phys. **A405**, 605 (1983).
- [36] A. Picklesimer, R. A. Rice, and R. Brandenburg, Phys. Rev. C **46**, 1178 (1992).
- [37] R. B. Wiringa, R. A. Smith, and T. L. Ainsworth, Phys. Rev. C **29**, 1207 (1984).
- [38] B. L. Friman, V. R. Pandharipande, and R. B. Wiringa, Phys. Rev. Lett. **51**, 763 (1983).
- [39] A. Akmal and V. R. Pandharipande, Phys. Rev. C **56**, 2261 (1997).
- [40] R. B. Wiringa in *Recent Progress in Many-Body Theories*, ed. H. Kümmel and M. L. Ristig (Springer-Verlag, Berlin, 1984)
- [41] F. Ajzenberg-Selove, Nucl. Phys. **A490**, 1 (1988).
- [42] D. R. Tilley, H. R. Weller, and H. H. Hasan, Nucl. Phys. **A474**, 1 (1987).
- [43] D. R. Tilley, H. R. Weller, and G. M. Hale, Nucl. Phys. **A541**, 1 (1992).
- [44] D. R. Tilley, C. M. Cheves, J. L. Godwin, G. M. Hale, H. M. Hofmann, J. H. Kelley, G. Sheu, and H. R. Weller, TUNL preprint “Energy Levels of Light Nuclei  $A = 5,6,7$ ” (2001).
- [45] H. De Vries, C. W. De Jager, and C. De Vries, At. Data Nucl. Data Tables **36**, 495 (1987).
- [46] A. A. Korshennikov *et al.*, Phys. Lett. B **316**, 38 (1993); W. von Oertzen *et al.*, Nucl. Phys. **A588**, 129c (1995); Th. Stolla *et al.*, Z. Phys. A **356**, 233 (1996).
- [47] D. Shiner, R. Dixson, and V. Vedantham, Phys. Rev. Lett. **74**, 3553 (1995).
- [48] P. Raghavan, At. Data Nucl. Data Tables **42**, 189 (1989); N. Stone, [www.nndc.bnl.gov/nndc/stone\\_moments/moments.html](http://www.nndc.bnl.gov/nndc/stone_moments/moments.html) (1997).
- [49] P. A. Whitlock, D. M. Ceperley, G. V. Chester, and M. H. Kalos, Phys. Rev. B **19**, 5598 (1979).
- [50] S. C. Pieper, R. B. Wiringa, and V. R. Pandharipande, Phys. Rev. C **46**, 1741 (1992).
- [51] S. C. Pieper and V. R. Pandharipande, Phys. Rev. Lett. **70**, 2541 (1993).
- [52] L. E. Marcucci, D. O. Riska, and R. Schiavilla, Phys. Rev. C **58**, 3069 (1998).
- [53] A. Nogga, D. Hüber, H. Kamada, and W. Glöckle, Phys. Lett. B **409**, 19 (1997).
- [54] G. E. Brown, W. Weise, G. Baym, and J. Speth, Comments Nucl. Part. Phys. **17**, 39 (1987).
- [55] J. L. Forest, private communication (1999).
- [56] V. R. Pandharipande, Nucl. Phys. **A645**, 157c (1999).
- [57] V. R. Pandharipande, Proc. of XVI Int. Conf. on Few Body Problems, Taipei (2000), to be published in Nucl. Phys.
- [58] A. Kievsky, Phys. Rev. C **60**, 034001 (1999).
- [59] H. Witała, W. Glöckle, D. Hüber, J. Golak, and H. Kamada, Phys. Rev. Lett. **81**, 1183 (1998).
- [60] H. Sakai *et al.*, Phys. Rev. Lett. **84**, 5288 (2000).
- [61] R. V. Cadman *et al.*, Phys. Rev. Lett. **86**, 967 (2001).

TABLES

TABLE I. Three-body potential parameters used in this paper. Parameters that were not varied in fitting the data are marked with an \*.

Model	$c$ fm <sup>-2</sup>	$A_{2\pi}^{PW}$ MeV	$A_{2\pi}^{SW}$ MeV	$A_{3\pi}^{\Delta R}$ MeV	$A_R$ MeV	$A_W$ MeV	$A_R^*$ MeV
UIX	2.1*	-0.0293	-	-	0.00480	0.*	0.00291
IL1	2.1*	-0.0385	0.0*	0.0026*	0.00705*	0.*	0.00491
IL2	2.1*	-0.037	-1.0*	0.0026	0.00705	0.*	0.00493
IL3	1.5	-0.07*	-1.0*	0.0065	0.032	0.*	0.02562
IL4	2.1*	-0.028*	-1.0*	0.0021	0.0039	0.*	0.00196
IL5	2.1*	-0.03	-1.0*	0.0021*	0.002*	210	0.0

TABLE II. Experimental and GFMC energies (in MeV) of particle-stable or narrow-width nuclear states and of neutron drops. Monte Carlo statistical errors in the last digits are shown in parentheses. The final column gives experimental widths in keV.

	AV8'	AV18	UIX	IL1	IL2	IL3	IL4	IL5	Expt.	$\Gamma$
<sup>3</sup> H( $\frac{1}{2}^+$ )	-7.76(1)	-7.61(1)	-8.46(1)	-8.43(1)	-8.43(1)	-8.41(1)	-8.44(1)	-8.41(1)	-8.48	
<sup>3</sup> He( $\frac{1}{2}^+$ )	-7.02(1)	-6.87(1)	-7.71(1)	-7.68(1)	-7.67(1)	-7.66(1)	-7.69(1)	-7.66(1)	-7.72	
<sup>4</sup> He( $0^+$ )	-25.14(2)	-24.07(4)	-28.33(2)	-28.38(2)	-28.37(3)	-28.24(3)	-28.35(2)	-28.23(2)	-28.30	
<sup>6</sup> He( $0^+$ )	-25.20(6)	-23.9(1)	-28.1(1)	-29.4(1)	-29.4(1)	-29.3(2)	-29.3(1)	-29.5(1)	-29.27	
<sup>6</sup> He( $2^+$ )	-23.18(6)	-21.8(1)	-26.3(1)	-27.2(1)	-27.1(1)	-27.8(1)	-27.4(1)	-27.3(1)	-27.47	113
<sup>6</sup> Li( $1^+$ )	-28.19(5)	-26.9(1)	-31.1(1)	-31.9(1)	-32.3(1)	-32.2(1)	-32.0(1)	-32.1(1)	-31.99	
<sup>6</sup> Li( $3^+$ )	-24.98(5)	-23.5(1)	-28.1(1)	-30.1(2)	-30.1(2)	-30.0(2)	-29.8(2)	-29.8(2)	-29.80	24
<sup>7</sup> He( $\frac{3}{2}^-$ )	-22.82(10)	-21.2(2)	-25.8(2)	-29.3(3)	-29.2(3)	-29.3(3)	-29.3(3)	-29.2(2)	-28.82	160
<sup>7</sup> Li( $\frac{3}{2}^-$ )	-33.56(6)	-31.6(1)	-37.8(1)	-39.4(2)	-39.6(2)	-39.3(2)	-39.5(2)	-39.3(2)	-39.24	
<sup>7</sup> Li( $\frac{1}{2}^-$ )	-33.17(7)	-31.1(2)	-37.5(2)	-39.2(2)	-39.1(2)	-38.7(2)	-39.0(2)	-39.0(2)	-38.77	
<sup>7</sup> Li( $\frac{7}{2}^-$ )	-28.41(6)	-26.4(1)	-32.1(1)	-34.5(3)	-34.4(3)	-34.0(2)	-34.5(2)	-34.2(3)	-34.61	93
<sup>8</sup> He( $0^+$ )	-23.8(1)	-21.6(2)	-27.2(2)	-30.5(3)	-31.3(3)	-32.0(4)	-31.9(4)	-31.0(2)	-31.41	
<sup>8</sup> Li( $2^+$ )	-34.2(1)	-31.8(3)	-38.0(2)	-41.8(3)	-42.2(2)	-41.2(3)	-42.0(3)	-42.5(3)	-41.28	
<sup>8</sup> Li( $1^+$ )	-33.9(1)	-31.6(2)	-37.4(2)	-40.5(3)	-40.5(3)	-40.2(3)	-40.9(3)	-40.9(3)	-40.30	
<sup>8</sup> Li( $3^+$ )	-31.4(1)	-28.9(2)	-35.3(2)	-39.3(3)	-39.1(3)	-39.5(4)	-39.3(3)	-39.2(3)	-39.02	33
<sup>8</sup> Li( $4^+$ )	-28.1(1)	-25.5(2)	-31.7(2)	-34.9(3)	-35.0(3)	-34.7(3)	-35.2(3)	-34.9(3)	-34.75	35
<sup>8</sup> Be( $0^+$ )	-47.9(1)	-45.6(3)	-54.4(2)	-57.2(4)	-56.6(4)	-55.6(4)	-56.5(3)	-55.7(3)	-56.50	
<sup>8</sup> Be( $1^+$ )	-32.8(2)	-30.9(3)	-36.3(3)	-37.8(2)	-37.6(2)	-37.3(3)	-38.8(3)	-38.9(4)	-38.35	138
<sup>7</sup> n( $\frac{1}{2}^-$ )	-33.78(4)	-33.47(5)	-33.2(1)	-36.0(2)	-35.8(2)	-36.6(3)	-35.2(3)	-35.3(3)		
<sup>7</sup> n( $\frac{3}{2}^-$ )	-32.25(4)	-31.82(5)	-31.7(1)	-33.2(2)	-33.0(2)	-33.0(3)	-32.9(3)	-33.1(2)		
<sup>8</sup> n( $0^+$ )	-39.73(6)	-39.21(8)	-37.8(1)	-41.3(3)	-41.1(3)	-40.7(2)	-40.7(3)	-40.7(2)		

TABLE III. Average deviations (in MeV) from experimental energies. For each Hamiltonian, the average signed deviation, average magnitude of deviation and rms deviation are shown for the 17 “narrow” states given in Table II (Only  ${}^3\text{He}$  energies are used for  $A = 3$ ).

Model	Average Deviation	Average  Deviation	rms Deviation
AV8'	5.52(2)	5.52	5.83
AV18	7.32(5)	7.32	7.72
AV18/UIX	2.02(4)	2.02	2.34
AV18/IL1	-0.09(6)	0.31	0.38
AV18/IL2	-0.10(6)	0.28	0.36
AV18/IL3	0.04(7)	0.31	0.44
AV18/IL4	-0.21(6)	0.24	0.33
AV18/IL5	-0.12(6)	0.34	0.46

TABLE IV. Average deviations (in MeV) from experimental excitation energies for the 8 “narrow” excited states. As in Table III, but for excitation energies rather than total energies.

Model	Average Deviation	Average  Deviation	rms Deviation
AV8'	-0.23(5)	0.83	1.20
AV18	-0.22(10)	0.90	1.36
AV18/UIX	0.17(8)	0.41	0.53
AV18/IL1	0.29(13)	0.44	0.53
AV18/IL2	0.53(12)	0.53	0.61
AV18/IL3	0.03(14)	0.24	0.34
AV18/IL4	0.09(12)	0.20	0.25
AV18/IL5	0.27(13)	0.66	0.79

TABLE V. Ground-state expectation values of the two-body potential and  $\langle K + v_{ij} \rangle$  (in MeV) for the AV8', AV18, AV18/UIX, and AV18/IL2 Hamiltonians.

	AV8'	AV18	AV18/UIX		AV18/IL2		
	$v_{ij}$	$v_{ij}$	$K + v_{ij}$	$v_{ij}$	$K + v_{ij}$	$v_{ij}$	$K + v_{ij}$
$^3\text{H}$	-54.9(2)	-54.8(2)	-7.605(5)	-58.7(2)	-7.27(1)	-58.6(2)	-6.97(1)
$^3\text{He}$	-53.4(2)	-53.3(2)	-6.882(5)	-57.1(2)	-6.54(1)	-56.7(2)	-6.27(1)
$^4\text{He}$	-126.(1)	-124.9(7)	-24.07(4)	-135.9(5)	-21.98(6)	-136.4(5)	-19.99(8)
$^6\text{He}$	-155.(1)	-153.(1)	-23.89(8)	-164.(1)	-21.1(2)	-171.(2)	-17.9(3)
$^6\text{Li}$	-174.(1)	-173.(1)	-26.9(1)	-182.(1)	-23.8(2)	-187.(2)	-21.2(3)
$^7\text{Li}$	-221.(2)	-219.(2)	-31.6(1)	-225.(2)	-28.7(2)	-232.(3)	-25.1(5)
$^8\text{He}$	-193.(3)	-191.(3)	-21.6(2)	-194.(1)	-19.1(2)	-218.(3)	-15.(1)
$^8\text{Li}$	-249.(4)	-247.(3)	-31.8(3)	-255.(2)	-27.8(3)	-278.(2)	-21.6(4)
$^8\text{Be}$	-287.(3)	-284.(3)	-45.6(3)	-297.(2)	-39.6(4)	-303.(3)	-35.5(8)
$^7\text{n}$	-54.8(7)	-54.5(7)	-33.47(5)	-54.2(8)	-33.86(9)	-59.(1)	-32.2(4)
$^8\text{n}$	-69.8(6)	-69.3(6)	-39.21(8)	-65.9(8)	-38.8(1)	-73.(1)	-38.2(5)

TABLE VI. Total three-nucleon potential energies (in MeV) for the AV18/UIX and Illinois Hamiltonians.

	AV18/UIX	AV18/IL1	AV18/IL2	AV18/IL3	AV18/IL4	AV18/IL5
$^3\text{H}$	-1.19(1)	-1.46(1)	-1.46(1)	-1.65(1)	-1.25(1)	-1.24(1)
$^3\text{He}$	-1.17(1)	-1.44(1)	-1.41(1)	-1.64(1)	-1.22(1)	-1.24(1)
$^4\text{He}$	-6.35(5)	-8.4(1)	-8.38(7)	-10.02(7)	-7.18(6)	-7.24(5)
$^6\text{He}$	-7.0(1)	-11.3(2)	-11.5(3)	-14.1(3)	-9.8(2)	-9.9(2)
$^6\text{Li}$	-7.3(2)	-11.2(3)	-11.1(3)	-13.6(3)	-9.6(2)	-10.2(2)
$^7\text{Li}$	-9.1(2)	-13.8(4)	-14.5(4)	-16.9(4)	-12.8(4)	-13.4(4)
$^8\text{He}$	-8.0(2)	-15.5(5)	-16.3(5)	-19.7(6)	-16.(1)	-14.7(3)
$^8\text{Li}$	-10.2(2)	-19.3(5)	-20.6(4)	-24.9(6)	-18.2(4)	-17.3(5)
$^8\text{Be}$	-14.9(3)	-20.8(7)	-21.(1)	-25.1(8)	-19.0(4)	-19.4(5)
$^7\text{n}$	0.69(4)	-3.8(3)	-3.6(3)	-4.8(4)	-2.5(3)	-2.5(4)
$^8\text{n}$	1.01(6)	-3.1(4)	-3.0(4)	-3.7(3)	-2.8(3)	-1.9(2)

TABLE VII. Contributions of various three-body potential terms (in MeV) evaluated for the AV18/IL2 Hamiltonian.

	$V^{2\pi,A}$	$V^{2\pi,C}$	$V^{2\pi,SW}$	$V^{3\pi,SS}$	$V^{3\pi,AA}$	$V^R$
${}^3\text{H}$	-1.78(1)	-1.082(9)	-0.119(1)	0	0.182(3)	1.34(1)
${}^3\text{He}$	-1.72(1)	-1.045(8)	-0.115(1)	0	0.176(3)	1.29(1)
${}^4\text{He}$	-9.76(8)	-5.85(5)	-0.652(5)	0	0.63(1)	7.26(7)
${}^6\text{He}$	-12.2(3)	-7.3(1)	-0.74(2)	-1.33(6)	0.42(4)	9.6(3)
${}^6\text{Li}$	-11.9(2)	-7.2(1)	-0.72(2)	-0.81(4)	0.37(4)	9.1(2)
${}^7\text{Li}$	-15.4(4)	-9.3(2)	-0.91(3)	-1.61(9)	0.5(1)	12.3(4)
${}^8\text{He}$	-15.6(4)	-9.1(2)	-0.88(3)	-4.5(2)	0.44(7)	13.3(4)
${}^8\text{Li}$	-20.7(3)	-12.2(2)	-1.26(2)	-4.4(1)	0.55(5)	17.4(3)
${}^8\text{Be}$	-23.1(6)	-14.0(3)	-1.38(4)	-1.6(1)	0.7(1)	18.3(6)
${}^7\text{n}$	-0.15(5)		0.08(1)	-5.4(3)	0	1.9(1)
${}^8\text{n}$	0.13(9)		0.18(1)	-5.9(4)	0	2.6(2)

TABLE VIII. Contributions of various three-body potential terms (in MeV) evaluated for the AV18/IL3 Hamiltonian.

	$V^{2\pi,A}$	$V^{2\pi,C}$	$V^{2\pi,SW}$	$V^{3\pi,SS}$	$V^{3\pi,AA}$	$V^R$
${}^3\text{H}$	-2.37(2)	-1.47(1)	-0.092(1)	0	0.217(3)	2.07(2)
${}^3\text{He}$	-2.35(2)	-1.46(1)	-0.091(1)	0	0.212(3)	2.04(2)
${}^4\text{He}$	-12.99(9)	-7.95(5)	-0.525(4)	0	0.54(1)	10.9(1)
${}^6\text{He}$	-16.4(3)	-9.9(2)	-0.61(1)	-1.9(1)	0.26(4)	14.5(3)
${}^6\text{Li}$	-16.2(3)	-9.9(2)	-0.59(1)	-1.31(6)	0.25(5)	14.2(4)
${}^7\text{Li}$	-20.9(5)	-12.8(3)	-0.73(2)	-2.32(9)	0.38(7)	19.5(6)
${}^8\text{He}$	-21.6(5)	-12.6(3)	-0.78(3)	-7.0(2)	0.16(9)	22.2(7)
${}^8\text{Li}$	-27.8(6)	-16.4(3)	-0.96(2)	-6.2(2)	0.13(9)	26.3(7)
${}^8\text{Be}$	-30.8(7)	-18.9(4)	-1.12(3)	-2.4(2)	0.7(1)	27.4(9)
${}^7\text{n}$	-0.13(8)		0.07(1)	-8.5(5)	0	3.8(2)
${}^8\text{n}$	0.52(8)		0.17(1)	-8.9(4)	0	4.5(1)



TABLE IX. Contributions of two-nucleon and three-nucleon pion and remainder potentials (in MeV) for the AV18/IL2 Hamiltonian.

	$v^\pi$	$v^R$	$V^{2\pi}$	$V^{3\pi}$	$V^R$
${}^3\text{H}$	-45.0(2)	-13.5(2)	-2.98(2)	0.182(3)	1.34(1)
${}^3\text{He}$	-44.4(2)	-12.4(2)	-2.88(2)	0.176(3)	1.29(1)
${}^4\text{He}$	-105.4(4)	-30.9(5)	-16.3(1)	0.63(1)	7.26(7)
${}^6\text{He}$	-127.(1)	-44.(2)	-20.3(4)	-0.91(6)	9.6(3)
${}^6\text{Li}$	-150.(1)	-38.(2)	-19.8(4)	-0.44(5)	9.1(2)
${}^7\text{Li}$	-178.(2)	-54.(3)	-25.6(6)	-1.1(1)	12.3(4)
${}^8\text{He}$	-153.(1)	-66.(3)	-25.6(6)	-4.0(2)	13.3(4)
${}^8\text{Li}$	-211.(1)	-67.(2)	-34.2(5)	-3.8(1)	17.4(3)
${}^8\text{Be}$	-234.(2)	-69.(3)	-38.5(9)	-0.9(2)	18.3(6)
${}^7\text{n}$	-10.11(9)	-49.(1)	-0.07(5)	-5.4(3)	1.9(1)
${}^8\text{n}$	-12.0(1)	-61.(1)	0.31(9)	-5.9(4)	2.6(2)

TABLE X. Isovector and isotensor energies ( $a_{A,T}^{(n)}$  in keV) for isomultiplets.

$A$	$T$	$n$	AV18	AV18/UIX	AV18/IL1	AV18/IL2	AV18/IL3	AV18/IL4	AV18/IL5	Expt.
3	$\frac{1}{2}$	1	732(1)	762(1)	757(2)	757(1)	752(1)	760(2)	759(2)	764
3	$\frac{1}{2}$	1	723(2)	753(1)	748(2)	747(1)	746(1)	751(2)	750(2)	764
3	$\frac{1}{2}$	1	731(7)	753(8)	754(7)	763(7)	748(8)	754(7)	753(7)	764
6	1	1	1068(4)	1102(9)	1149(6)	1172(6)	1141(5)	1147(6)	1179(6)	1173
7	$\frac{1}{2}$	1	1586(7)	1565(7)	1613(8)	1588(7)	1554(9)	1609(8)	1610(8)	1644
8	2	1	1457(7)	1488(5)	1581(7)	1622(8)	1631(9)	1670(9)	1637(6)	1659
8	1	1	1636(9)	1672(7)	1762(8)	1810(6)	1759(8)	1837(7)	1774(9)	1770
6	1	2		251(18)	275(13)	293(13)	266(16)	287(18)	280(17)	223
8	2	2		158(4)	170(4)	180(5)	180(5)	188(5)	175(3)	153
8	1	2		135(7)	135(12)	143(8)	99(12)	148(10)	156(12)	145

TABLE XI. Various contributions to the isovector and isotensor energies (in keV) computed with AV18/IL2. The definitions of the contributions are given in the text.

$A$	$T$	$n$	$K^{CSB}$	$v_{C1}(pp)$	$v^{\gamma,R}$	$v^{CSB} + v^{CD}$	Total	Expt.
3	$\frac{1}{2}$	1	14(0)	649(1)	29(0)	64(0)	757(1)	764
6	1	1	16(0)	1091(5)	18(0)	47(1)	1172(6)	1173
7	$\frac{1}{2}$	1	22(0)	1447(6)	40(0)	79(2)	1588(7)	1644
8	2	1	18(0)	1528(7)	17(0)	59(1)	1622(8)	1659
8	1	1	23(0)	1686(5)	24(0)	76(1)	1810(6)	1770
6	1	2		166(1)	19(0)	107(13)	293(13)	223
8	2	2		136(1)	6(0)	38(5)	180(5)	153
8	1	2		141(1)	4(0)	-3(8)	143(8)	145

TABLE XII. Experimental and computed energies (in MeV) of “wide” or experimentally unknown states. The experimental widths (in keV) of the states are also given.

	AV8'	AV18	UIX	IL1	IL2	IL3	IL4	IL5	Expt.	$\Gamma$
${}^5\text{He}(\frac{3}{2}^-)$	-23.85(4)	-22.47(9)	-26.9(1)	-27.7(1)	-27.7(1)	-27.4(1)	-27.5(1)	-27.4(1)	-27.52(2)	650
${}^5\text{He}(\frac{1}{2}^-)$	-23.17(3)	-21.9(1)	-25.8(1)	-26.5(1)	-26.4(1)	-26.3(1)	-26.1(1)	-26.0(1)	-26.32(20)	5500
${}^6\text{He}(1^+)$	-21.58(4)	-20.2(1)	-24.4(1)	-24.7(1)	-24.5(1)	-24.2(1)	-24.1(2)	-24.1(1)		
${}^6\text{Li}(2^+)$	-24.12(4)	-22.7(1)	-27.2(1)	-27.9(1)	-27.9(1)	-27.7(2)	-27.9(1)	-27.8(1)	-27.68(2)	1700
${}^7\text{He}(\frac{1}{2}^-)$	-22.01(10)	-20.8(2)	-24.3(2)	-26.6(2)	-26.5(2)	-26.3(2)	-26.1(2)	-26.3(2)		
${}^7\text{He}(\frac{5}{2}^-)$	-20.81(10)	-19.2(2)	-23.2(2)	-24.7(3)	-24.4(3)	-25.0(2)	-25.0(2)	-25.0(2)	-25.92(30)	2200
${}^7\text{Li}(\frac{3}{2}^-)$	-27.52(5)	-25.7(1)	-31.3(1)	-32.3(2)	-32.2(2)	-32.0(2)	-32.1(2)	-32.3(2)	-32.56(5)	875
${}^8\text{He}(2^+)$	-21.39(8)	-19.6(2)	-24.1(2)	-26.8(3)	-26.6(3)	-26.2(3)	-27.2(3)	-26.6(3)	-27.82(5)	630
${}^8\text{He}(1^+)$	-21.2(1)	-19.6(2)	-22.7(2)	-26.0(3)	-25.8(3)	-26.2(3)	-25.8(3)	-25.8(3)		
${}^8\text{Li}(0^+)$	-33.5(1)	-31.3(2)	-36.1(2)	-38.4(3)	-38.4(3)	-37.2(4)	-37.8(4)	-38.3(4)		
${}^8\text{Be}(2^+)$	-45.6(1)	-42.7(3)	-51.5(2)	-53.6(3)	-53.5(3)	-52.4(3)	-53.1(3)	-53.2(3)	-53.46(3)	1500
${}^8\text{Be}(4^+)$	-38.7(1)	-36.2(2)	-44.9(2)	-45.5(3)	-45.4(3)	-45.0(3)	-45.4(3)	-45.9(3)	-45.10(30)	3500
${}^8\text{Be}(3^+)$	-31.2(2)	-29.3(3)	-34.9(3)	-37.2(3)	-37.1(3)	-36.9(3)	-38.0(4)	-37.2(3)	-37.26(3)	230

TABLE XIII. Computed and experimental spin-orbit splittings in MeV.

	$L$	$S$	AV8'	AV18	UIX	IL1	IL2	IL3	IL4	IL5	Expt	
${}^5\text{He}$	$\frac{1}{2}^- - \frac{3}{2}^-$	1	$\frac{1}{2}$	0.68(5)	0.6(1)	1.1(2)	1.2(2)	1.3(2)	1.1(2)	1.4(2)	1.3(2)	1.20
${}^6\text{Li}$	$2^+ - 3^+$	2	1	0.86(6)	0.8(1)	0.9(1)	2.2(2)	2.2(2)	2.4(2)	1.9(2)		2.12
${}^7\text{Li}$	$\frac{1}{2}^- - \frac{3}{2}^-$	1	$\frac{1}{2}$	0.39(9)	0.5(2)	0.3(2)	0.2(3)	0.6(3)	0.6(3)	0.4(3)	0.3(3)	0.47
${}^7\text{Li}$	$\frac{5}{2}^- - \frac{7}{2}^-$	3	$\frac{1}{2}$	0.89(8)	0.7(2)	0.8(2)	2.2(3)	2.2(3)	2.0(3)	2.4(3)	2.0(3)	2.05
${}^8\text{Li}$	$1^+ - 2^+$	1	1	0.3(2)	0.2(4)	0.6(2)	1.3(4)	1.7(4)	1.1(5)	1.1(4)	1.6(4)	0.98
${}^7\text{n}$	$\frac{3}{2}^- - \frac{1}{2}^-$	1	$\frac{1}{2}$	1.53(6)	1.65(7)	1.5(1)	2.8(3)	2.8(3)	3.6(4)	2.4(4)	2.3(3)	

TABLE XIV. RMS point proton and neutron radii in fm.

	AV8'		AV18/UIX		AV18/IL2		AV18/IL3		AV18/IL4		Expt
	$p$	$n$	$p$	$n$	$p$	$n$	$p$	$n$	$p$	$n$	
${}^3\text{H}$	1.66(0)	1.82(0)	1.59(0)	1.73(0)	1.59(0)	1.74(0)	1.60(0)	1.74(0)	1.59(0)	1.73(0)	1.60
${}^3\text{He}$	1.85(0)	1.68(0)	1.76(0)	1.61(0)	1.76(0)	1.61(0)	1.76(0)	1.61(0)	1.76(0)	1.61(0)	1.77
${}^4\text{He}$	1.50(0)	1.50(0)	1.44(0)	1.44(0)	1.45(0)	1.45(0)	1.46(0)	1.46(0)	1.44(0)	1.44(0)	1.47
${}^6\text{He}$	2.06(1)	3.07(1)	1.97(1)	2.94(1)	1.91(1)	2.82(1)	1.99(1)	2.97(1)	1.99(1)	2.96(1)	
${}^6\text{Li}$	2.50(1)	2.50(1)	2.57(1)	2.57(1)	2.39(1)	2.39(1)	2.44(1)	2.44(1)	2.38(1)	2.38(1)	2.43
${}^7\text{Li}$	2.29(1)	2.47(1)	2.33(1)	2.52(1)	2.25(1)	2.44(1)	2.32(1)	2.52(1)	2.26(1)	2.44(1)	2.27
${}^8\text{He}$	1.93(1)	3.22(2)	1.98(0)	3.17(1)	1.88(1)	2.96(1)	1.86(1)	2.92(1)	1.82(1)	2.88(1)	
${}^8\text{Li}$	2.31(1)	2.73(1)	2.19(1)	2.65(1)	2.09(1)	2.45(1)	2.11(1)	2.51(1)	2.07(1)	2.43(1)	
${}^8\text{Be}$	2.42(1)	2.42(1)	2.48(0)	2.48(0)	2.44(1)	2.44(1)	2.48(1)	2.48(1)	2.39(1)	2.39(1)	
${}^7\text{n}$		3.08(1)		3.09(1)		2.92(0)		2.85(1)		2.85(1)	
${}^8\text{n}$		2.98(0)		3.03(1)		2.92(0)		2.88(0)		2.88(1)	

TABLE XV. Isoscalar and isovector magnetic moments, calculated in impulse approximation, in nuclear magnetons.

	T	AV8'	UIX	IL2	IL3	IL4	Expt
Isoscalar							
$^3\text{He}-^3\text{H}$	$\frac{1}{2}$	0.408(0)	0.405(0)	0.403(0)	0.402(0)	0.404(0)	0.426
$^6\text{Li}$	0	0.823(1)	0.821(1)	0.817(1)	0.810(1)	0.819(1)	0.822
$^7\text{Be}-^7\text{Li}$	$\frac{1}{2}$	0.904(6)	0.90(1)	0.894(1)	0.895(1)	0.898(1)	0.929
$^8\text{B}-^8\text{Li}$	1	1.31(1)	1.307(2)	1.276(1)	1.287(1)	1.295(1)	1.345
Isovector							
$^3\text{He}-^3\text{H}$	$\frac{1}{2}$	-4.354(1)	-4.340(1)	-4.330(1)	-4.316(1)	-4.331(1)	-5.107
$^7\text{Be}-^7\text{Li}$	$\frac{1}{2}$	-3.92(1)	-3.96(1)	-3.93(1)	-3.84(1)	-3.96(1)	-4.654
$^8\text{B}-^8\text{Li}$	1	0.39(1)	0.40(2)	0.369(9)	0.34(1)	0.377(9)	-0.309

TABLE XVI. Quadrupole moments, calculated in impulse approximation, in fm<sup>2</sup>.

	AV8'	UIX	IL2	IL3	IL4	Expt
$^6\text{Li}$	-0.27(8)	-0.1(2)	-0.32(6)	-0.35(6)	0.27(5)	-0.083
$^7\text{Li}$	-3.6(1)	-4.5(1)	-3.6(1)	-3.4(1)	-3.9(1)	-4.06
$^7\text{Be}$	-6.4(1)	-7.5(1)	-6.1(1)	-5.4(1)	-6.6(1)	
$^8\text{Li}$	3.5(3)	3.0(1)	3.2(1)	3.2(1)	3.4(1)	3.19(7)
$^8\text{B}$	7.1(3)	8.2(1)	6.4(1)	5.6(1)	6.6(1)	6.8(2)

TABLE XVII. Expectation values of  $\delta v$  and the net change in the binding energy due to the boost correction (in MeV) for three of the Illinois Hamiltonians.

	$\delta v$			$\delta v + (V_{ijk}^* - V_{ijk})$		
	AV18/IL1	AV18/IL4	AV18/IL5	AV18/IL1	AV18/IL4	AV18/IL5
${}^3\text{H}(\frac{1}{2}^+)$	0.406(4)	0.394(4)	0.395(4)	0.000(8)	-0.001(8)	-0.012(8)
${}^3\text{He}(\frac{1}{2}^+)$	0.394(4)	0.382(4)	0.386(4)	-0.003(8)	0.001(8)	-0.005(8)
${}^4\text{He}(0^+)$	2.13(2)	2.09(2)	2.08(2)	-0.10(4)	-0.08(4)	-0.10(4)
${}^6\text{He}(0^+)$	2.81(9)	2.93(8)	2.83(8)	0.1(1)	0.1(1)	0.1(1)
${}^6\text{He}(2^+)$			2.78(8)			0.1(1)
${}^6\text{Li}(1^+)$	2.81(8)	2.96(9)	3.04(8)	0.2(1)	0.2(1)	0.2(1)
${}^7\text{Li}(\frac{3}{2}^-)$	3.9(1)	4.0(1)	3.8(1)	0.1(2)	0.4(2)	0.3(2)
${}^7\text{Li}(\frac{1}{2}^-)$			4.1(1)			0.4(2)
${}^7\text{Li}(\frac{7}{2}^-)$			4.1(1)			0.5(2)
${}^8\text{He}(0^+)$	4.2(1)	4.5(2)	4.5(1)	0.5(2)	0.0(2)	0.2(2)
${}^8\text{Li}(2^+)$	5.4(1)	5.9(2)	5.3(2)	0.3(2)	0.3(2)	0.3(2)
${}^8\text{Li}(1^+)$			5.2(2)			0.1(2)
${}^8\text{Li}(3^+)$			5.7(2)			0.2(3)
${}^8\text{Li}(4^+)$	5.0(1)		5.3(2)	0.7(2)		0.6(2)
${}^8\text{Be}(0^+)$	5.6(2)	5.6(2)	5.8(3)	0.1(3)	0.3(2)	0.3(4)
${}^8\text{Be}(1^+)$			5.3(2)			0.3(3)
${}^8\text{n}(0^+)$		1.25(4)	1.12(5)		0.61(5)	0.57(6)

## FIGURES

FIG. 1. Energies of ground or low-lying excited states of light nuclei computed with the AV18 and AV18/UIX interactions, compared to experiment. The light shading shows the Monte Carlo statistical errors. The dashed lines indicate the thresholds against breakup for each model or experiment.

FIG. 2. Three-body force Feynman diagrams. The first, a, is the Fujita-Miyazawa, b is two-pion S-wave, c and d are three-pion rings with one  $\Delta$  in intermediate states.

FIG. 3. Energies computed with the AV18/UIX, AV18/IL2, and AV18/IL4 Hamiltonians compared to experiment for narrow states. The light shading shows the Monte Carlo statistical errors. The dashed lines indicate the thresholds against breakup for each model or experiment.

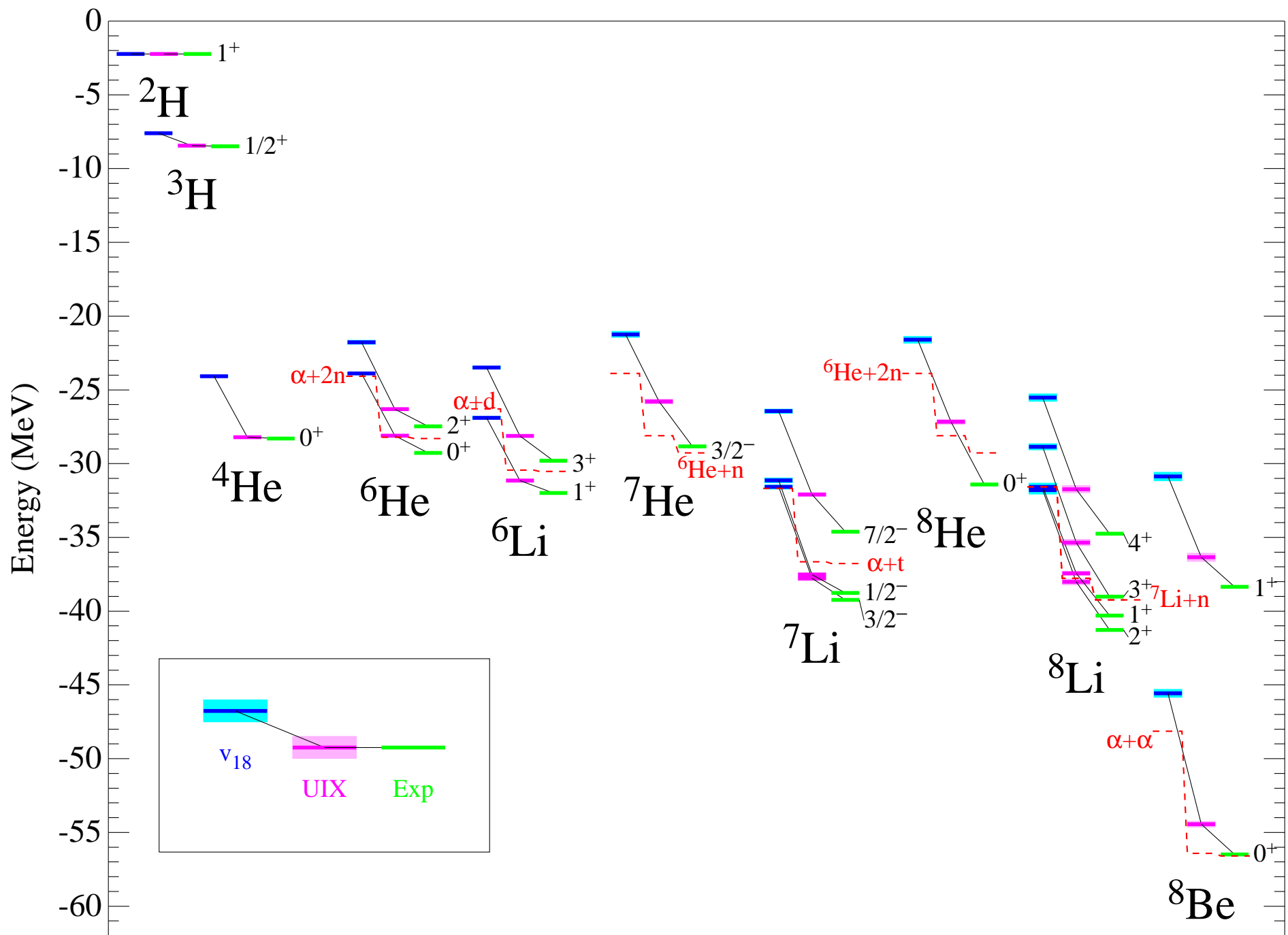
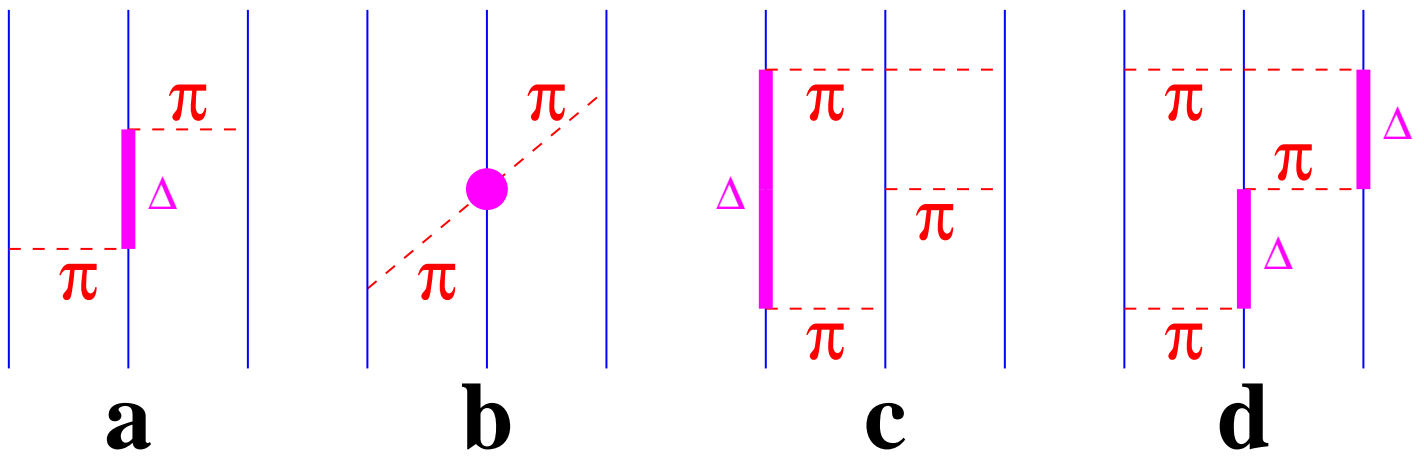


Fig. 1 (Pieper, et al.)

Fig. 2 (Pieper, et al.)



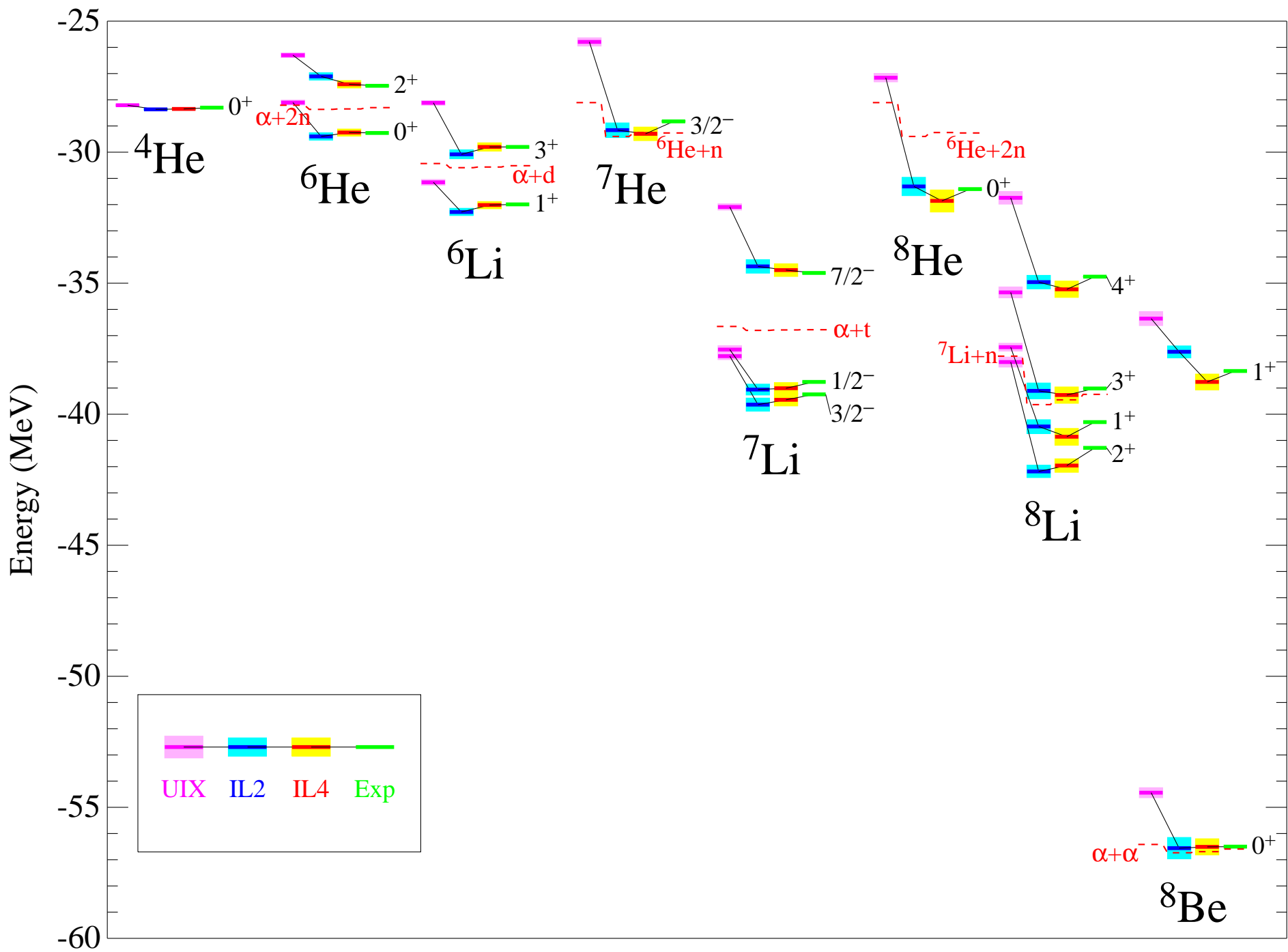


Fig. 3 (Pieper, et al.)